Journal of Medicinal Chemistry

Article

pubs.acs.org/jmc

Carbonylhydrazide-Based Molecular Tongs Inhibit Wild-Type and Mutated HIV-1 Protease Dimerization

Laure Dufau,[‡] Ana Sofia Marques Ressurreição,[†] Roberto Fanelli,[†] Nadjib Kihal,[†] Anamaria Vidu,[†] Thierry Milcent,[†] Jean-Louis Soulier,[†] Jordi Rodrigo,[†] Audrey Desvergne,[‡] Karine Leblanc,[†] Guillaume Bernadat,[†] Benoit Crousse,[†] Michèle Reboud-Ravaux,*[,‡] and Sandrine Ongeri*[,†]

[†]UMR−CNRS 8076, Molécules Fluorées et Chimie Médicinale, LabEx LERMIT, Faculté de Pharmacie, Université Paris-Sud 11, 5 rue J. B. Clément, 92296 Châtenay-Malabry Cedex, France

[‡]UPMC−UR4, Enzymologie Moléculaire et Fonctionnelle, Case 256, 7 Quai St. Bernard, 75251 Paris Cedex 05, France

Supporting Information

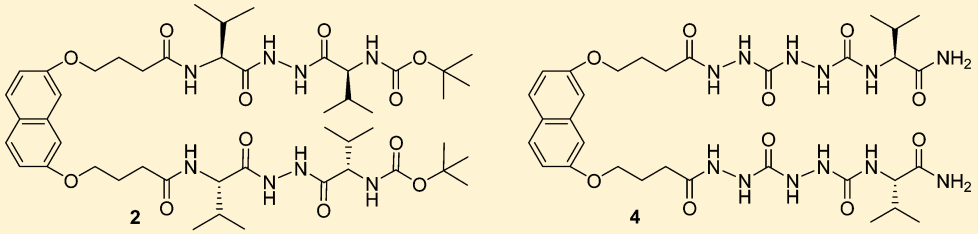

K_{id} (WT) = 50 nM
K_{id} (ANAM-11) = 80 nM

K_{id} (WT) = 700 nM
K_{id} (ANAM-11) = 800 nM

ABSTRACT: We have designed and synthesized new molecular tongs based on a rigid naphthalene scaffold and evaluated their antidimer activity on HIV-1 protease (PR). We inserted carbonylhydrazide and oligohydrazide (azatide) fragments into their peptidomimetic arms to reduce hydrophobicity and increase metabolic stability. These fragments are designed to disrupt the protein−protein interactions by reproducing the hydrogen bond pattern found in the antiparallel β-sheet formed between the *N*- and *C*-ends of the two monomers in the native PR. Kinetic analyses and fluorescent probe binding studies showed that several molecular tongs can inhibit PR dimerization. The best nonpeptidic molecular tongs to date were obtained with an inhibition constant K_{id} of 50 nM for PR and 80 nM for the multimutated protease ANAM-11. The PR inhibition was selective, the aspartic proteases renin and pepsin were not inhibited.

INTRODUCTION

The post-translational processing of virus polyproteins and the subsequent generation of the structural and functional proteins by human immunodeficiency virus type 1 (HIV-1) protease (PR) are essential steps in the maturation of HIV.[1] Inhibiting PR results in the production of an uninfectious virus.[2] The PR inhibitors (PIs) used in highly active antiretroviral therapy (HAART) target the PR active site where the two catalytic aspartic residues are located. The emergence of resistance to PIs due to several mutations within or outside the active site[3,4] has led to a search for alternative strategies. One of these is to prevent the essential dimerization process of PR because PR is a homodimeric aspartyl protease (99 residues per monomer) and each monomer contributes one catalytic aspartic residue. The dimeric enzyme is active, whereas the monomer is inactive. The PR homodimer is mainly stabilized by a four-stranded antiparallel β-sheet that involves the *N*-termini (H-Pro(1)-Gln(2)-Ile(3)-Thr(4)) and *C*-termini (Cys(95)-Thr(96)-Leu(97)-Asn(98)-Phe(99)-OH) of both monomers. These regions provide over 50% of the hydrogen bonds along the dimer interface[5] and contribute close to 75% of the total Gibbs free energy of PR dimerization.[6] Moreover, these areas appear to be free of mutations.[7] Dimerization inhibitors designed to target the PR termini β-sheet interface can block the formation of the homodimer or even disrupt it.[8,9] The dimerization inhibitors that target this β-sheet region are *C*-terminal and *N*-terminal mimetic peptides,[10−12] lipopeptides,[13−15] bicyclic guanidinium derivatives,[16] and cross-linked peptides with flexible[17] or semirigid spacers.[18] The recently approved PIs, tipranavir and darunavir, are active against HIV-1 PR variants that are resistant to many PIs and reportedly act as conventional protease inhibitors. They also block protease dimerization in cells but do not dissociate dimerized cellular protease.[19] Our strategy for inhibiting PR dimerization is to design molecular tongs using a rigid spacer as this provides an entropy benefit.[20−23] We previously described the design of organized molecular tongs based on a naphthalene or a quinoline scaffold in which two peptide strands were attached through a carboxypropyloxy linker to enable them to form an

Received: February 9, 2012
Published: July 17, 2012

   dx.doi.org/10.1021/jm300181j | *J. Med. Chem.* 2012, 55, 6762−6775

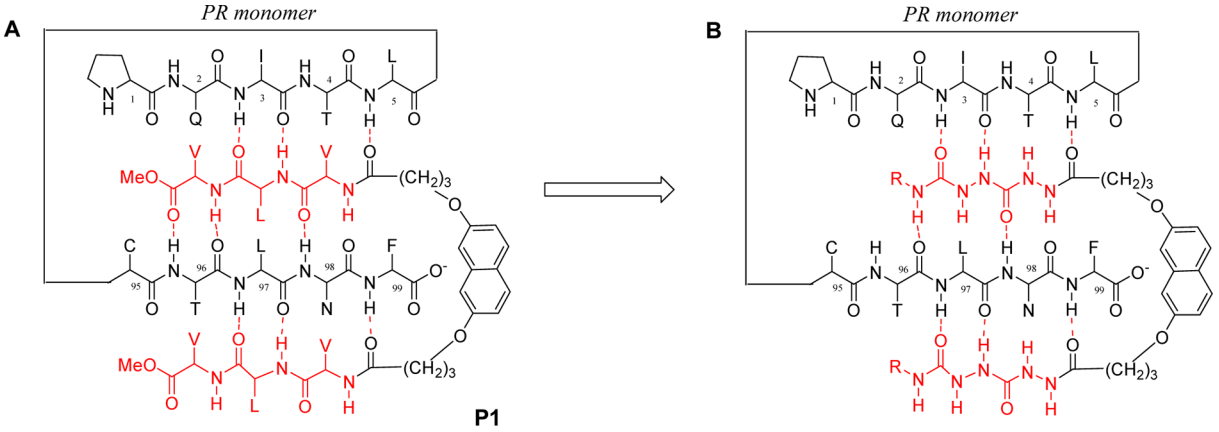

Figure 1. (A) Putative complexes between HIV-1 protease monomer and **P1** peptide molecular tong; (B) putative complexes between HIV-1 protease monomer and dihydrazido peptidomimetic molecular tongs.

antiparallel β-sheet with the *N*- and *C*-termini of one HIV-1 PR monomer (molecular tong **P1** in Figure 1A). Identical peptide strands led to efficient symmetrical antidimers, while non-identical peptides gave asymmetrical antidimers.[20,21] The next step was to replace one or two peptide fragments by peptidomimetic ones with keeping the same array of hydrogen bonds.[22,23] Inserting a 5-acetamido-2-methoxybenzohydrazide group into one strand (while the other strand remained a tripeptide) increased both the metabolic stability of the molecular tongs and their ability to inhibit wild-type (PR) and mutated HIV-1 proteases in vitro (K_{id} = 60 nM for PR and 100 nM for the multimutated protease ANAM-11).[22,23] We also inserted the 5-acetamido-2-methoxybenzydrazide group into both strands to produce the first nonpeptide molecular tongs.[23] However, these molecules were less efficient inhibitors of PR and mutated proteases (K_{id} up to 220 nM compared to 60 nM for the molecular tong with one tripeptide and one peptidomimetic strands[23]). One drawback of our previous peptide or peptidomimetic molecular tongs was that they were completely insoluble in water. We are now concerned with obtaining more efficient and more water-soluble nonpeptide molecular tongs. This report describes the design and synthesis of new molecular tongs containing the original carbonylhydrazide (CONHNHCO) peptidomimetic fragments and their ability to inhibit PR and two multimutated mutated HIV-1 proteases (Figure 2). These motifs were chosen because they are isosteric elements that can replace amino acid residues and introduce resistance to cleavage by peptidases.[24,25] Oligohydrazide derivatives have also been used in the self-assembly of hydrogen bond-mediated supramolecular systems to produce well-established structures.[26−28] However, the linear hydrogen-bonding properties of carbonylhydrazide and oligohydrazide peptidomimetics have not yet, to our knowledge, been exploited in the design of protein ligands and protein−protein interactions inhibitors. We postulated that these peptidomimetic elements would operate mainly by binding to the antiparallel β-sheet formed between the *N*- and *C*-ends of monomers and so disrupt dimers (Figure 1B). According to the number of fragments introduced, they may also modulate the balance between hydrophilicity and hydrophobicity and make peptides resistant to proteolytic cleavage of the newly designed molecular tongs. This report describes the most potent nonpeptide molecular tongs obtained to date as dimerization inhibitors of HIV-1 PR.

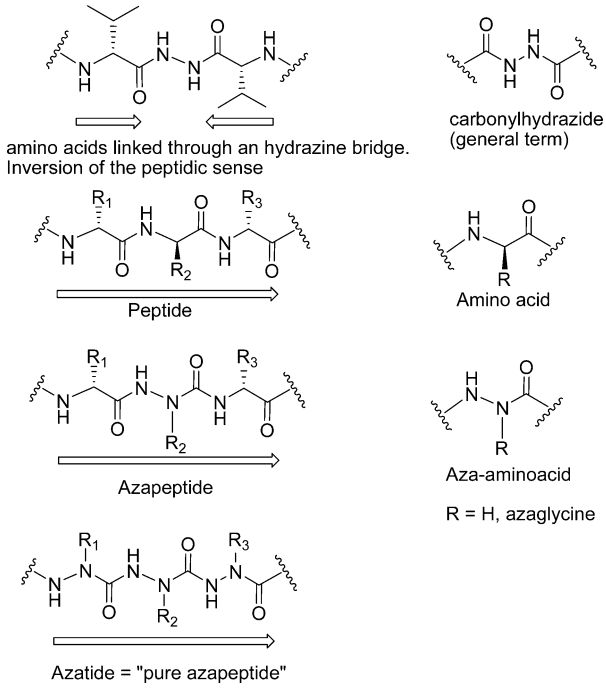

Figure 2. General structure of motifs inserted into one or two arms of molecular tongs.

All the molecular tongs were based on a naphthalene scaffold and the new strands, mimicking a tripeptidic sequence (except for molecule **6**), were anchored through a carboxypropyloxy linker. We made several changes to the structures of the strands. We first inserted one carbonylhydrazide motif by linking two Val residues through a hydrazine bridge, thus inverting the sense of the peptide arm (Figure 2). This new peptidomimetic was introduced into one or two strands (molecules **1** and **2**, respectively, Figure 3). As our goal was to decrease the peptide character and increase the water solubility of the molecular tongs, we then introduced two hydrazide moieties via an azatide (a sequence of aza amino acids) by inserting two azaglycines into the peptidomimetic arms (Figure 2). The azatide moieties were first directly attached to the carboxypropyloxy link (in molecules **3**−**6**, Figure 3). A Val and a β-Ala amino acid residue were coupled at the *C*-terminus of the arm in molecules **3** and **4** and in molecule **5**, respectively. Second, the azatide moieties were

dx.doi.org/10.1021/jm300181j | J. Med. Chem. 2012, 55, 6762−6775

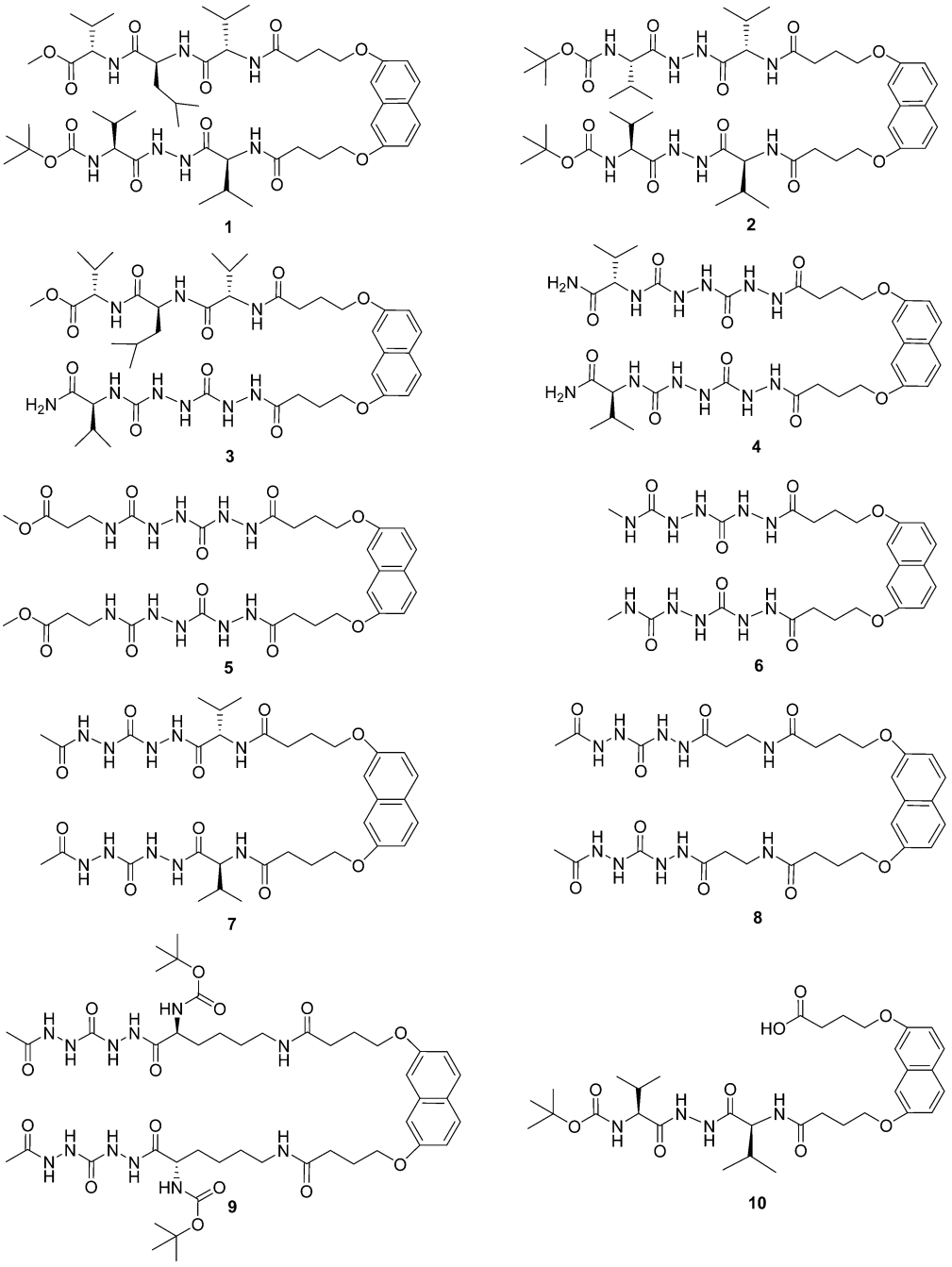

Figure 3. Structures of molecular tongs **1**−**10**.

attached to the carboxypropyloxy link through an amino acid residue at the *N*-terminus of the arm (in molecules **7**−**9**, Figure 3). The azatide moiety was coupled to Val in molecule **7**, *β*-Ala in molecule **8**, and the *ε*-amino group of an *α*-NH_2 protected Lys residue in molecule **9**. The presence of the *β*-Ala residue (**8**) or *ε*-amino-linked Lys residue (**9**) introduced flexibility in the arm (Figure 3), as reported for molecular tongs having the 5-acetamido-2-methoxybenzohydrazide derivative unit.[22,23] We also designed a shorter dihydrazide-based peptidomimetic unit in which the third terminal amino acid residue was replaced by a methylamine group (molecule **6**) (Figure 3). We also evaluated the capacity of molecule **10**, which possesses only one peptidomimetic arm (Figure 3) to inhibit PR dimerization, to confirm that only molecular tongs with two arms attached to on the naphthalene scaffold are efficient inhibitors.

CHEMISTRY

The synthesis of the peptidomimetic **14** (to be introduced in molecular tongs **1**, **2**, and **10**) is described is Scheme 1 and started with the preparation of the intermediate *Z*-Val-NHNHBoc **11**. **11** was obtained by coupling *Z*-Val-OH to *tert*-butyl carbazate, using 1-ethyl-3-(3-dimethylaminopropyl) carbodiimide (EDCI) and *N*-hydroxybenzotriazole (HOBt) as coupling agents in good yield (88%) (Scheme 1). Hydrogenolysis of the benzyl carbamate of **11** gave **12** in good yield (96%). Acidic cleavage of the *tert*-butyl carbamate of **11** and its coupling to *N*-Boc-Val-OH gave compound **13**. Benzyl carbamate hydrogenolysis of **13** gave the deprotected peptidomimetic strand **14** with a satisfactory yield (71%) (Scheme 1).

dx.doi.org/10.1021/jm300181j | *J. Med. Chem.* 2012, 55, 6762−6775

Scheme 1. Synthesis of Peptidomimetics Containing Strands 12 and 14[a]

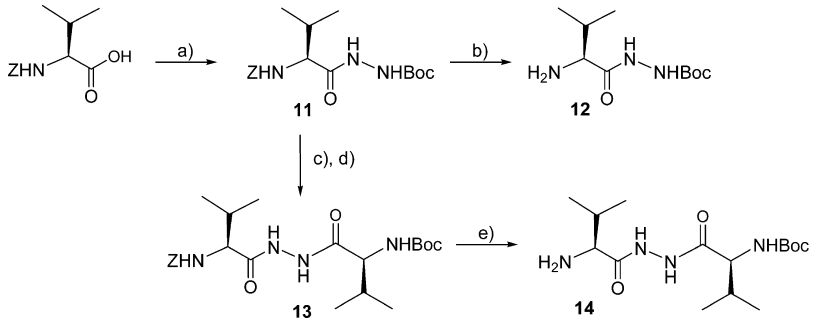

[a](a) $BocNHNH_2$, EDCI, HOBt, DIPEA, CH_2Cl_2, room temp; (b) H_2, 10% Pd/C, MeOH, room temp; (c) HCl/dioxane 4 M, dioxane, room temp; (d) *N*-Boc-Val-OH, EDCI, HOBt, DIPEA, DMF, room temp; (e) H_2, 10% Pd/C, MeOH, room temp.

Scheme 2. Synthesis of Peptidomimetics Containing Strands 19, 21, and 23[a]

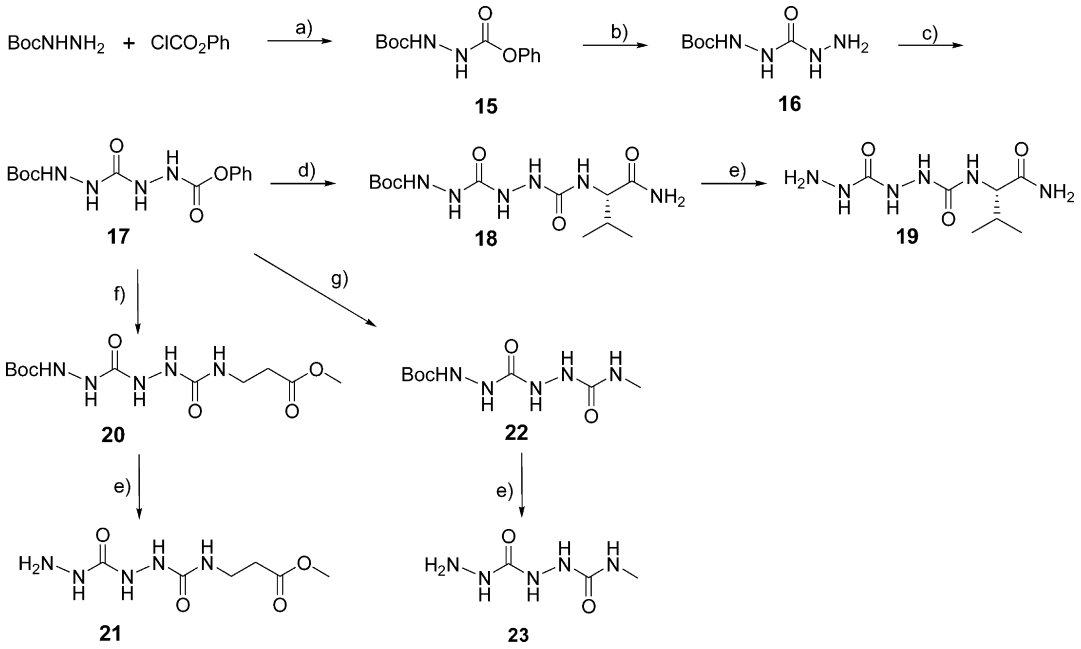

[a](a) Pyridine, CH_2Cl_2, room temp; (b) $H_2NNH_2{\cdot}H_2O$, MeOH; (c) $ClCO_2Ph$, pyridine, THF, room temp; (d) HCl·H-Val-NH_2, Et_3N, AcCN, room temp; (e) TFA/CH_2Cl_2 (1:1, v/v), room temp; (f) HCl·NH_2CH_3, Et_3N, AcCN, room temp; (g) HCl·H-*β*-Ala-OMe, Et_3N, AcCN, room temp.

The procedure designed to obtain the new peptidomimetic arms involved the synthesis of a dihydrazide motif **16** that was common to all azatide-based arms (molecules **3**–**9**). Thus, compound **15** was prepared in 97% yield by reacting the commercially available compounds *tert*-butyl carbazate and phenyl chloroformate in dichloromethane in the presence of pyridine (Scheme 2).[29] Treatment of **15** with hydrazine hydrate gave the intermediate **16** in 72% yield.[29] Compound **16** was then treated with phenyl chloroformate in THF, in the presence of pyridine, to give **17** in good yield (91%). Compound **17** was then coupled to HCl·H-Val-NH_2 to give the Boc-protected peptidomimetic arm **18** in good yield (93%). Classical acid hydrolysis of **18** gave the new peptidomimetic arm **19** (Scheme 2). Compound **17** was also coupled to methyl amine to give **20** (yield 70%) and to HCl·H-*β*-Ala-OMe to give **22** (yield 67%). Acid cleavage of the *tert*-butyl carbamates gave the new peptidomimetic arms **21** and **23** (Scheme 2).

Compound **16** was acetylated to give **24** in good yield (96%) (Scheme 3). Acid cleavage of the *tert*-butyl carbamate gave the common intermediate **25**, which was coupled to *N*-Boc-Val-OH, *N*-Boc-*β*-Ala-OH, or *Nα*-Boc-*Nε*-*Z*-Lys-OH, using *O*-benzotriazole-*N*,*N*,*N*′,*N*′-tetramethyl-uronium-hexafluoro-phosphate (HBTU) and HOBt as coupling agents to give compounds **26**, **28**, or **30** in modest yields (46%, 12%, or 30%). These modest yields may be partly due to the hydrophilic compounds **26**, **28**, and **30** remaining in the aqueous phase during the workup of the coupling reaction and consequently being very difficult to extract with organic solvents. The acid hydrolysis of **26** and **28** gave the deprotected peptidomimetic strands **27** and **29**, and benzyl carbamate hydrogenolysis of **30** gave the peptidomimetic strand **31** (Scheme 3).

The molecular tongs **1** was synthesized in three steps from 4-[7-(3-carboxy-propoxy)naphthalene-2-yloxy]butyryl-Val-Leu-Val-OMe **32**[21] (Scheme 4). **32** was first condensed with Val-NHNHBoc **12** to form the intermediate **33** in 76% yield. *tert*-Butyl carbamate cleavage of **33** was then followed by coupling to *N*-Boc-Val-OH to give molecular tongs **1** in satisfactory yield (55%). The molecular tongs **3** was synthesized directly by condensing 4-[7-(3-carboxy-propoxy)naphthalene-2-yloxy]-

dx.doi.org/10.1021/jm300181j | *J. Med. Chem.* 2012, 55, 6762–6775

Scheme 3. Synthesis of Peptidomimetics Containing Strands 27, 29, and 31[a]

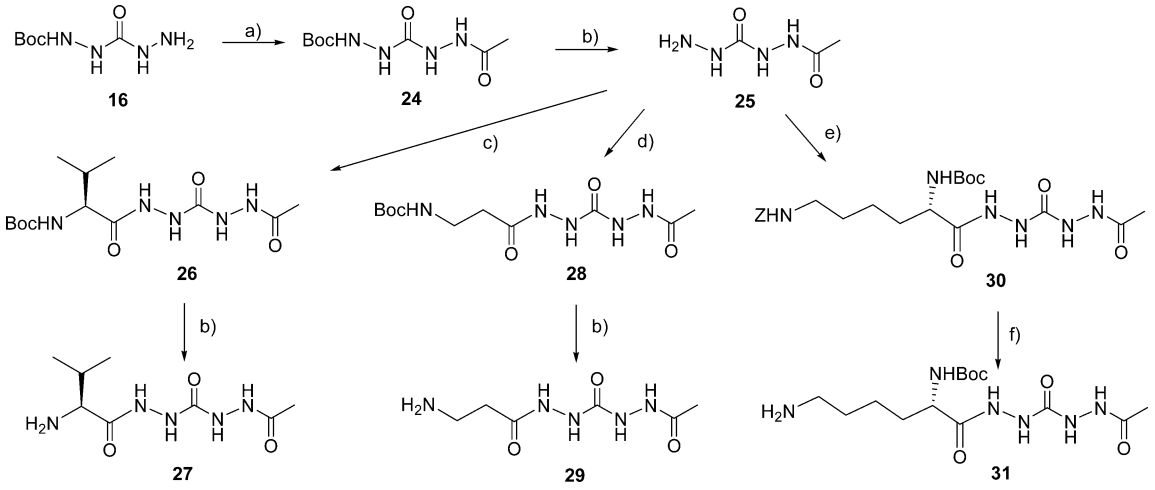

[a](a) Ac_2O, THF, reflux; (b) HCl/dioxane 4M, dioxane, room temp; (c) *N*-Boc-Val-OH, HBTU, HOBt, DIPEA, DMF, room temp; (d) *N*-Boc-*β*-Ala-OH, HBTU, HOBt, DIPEA, DMF, room temp; (e) *Nα*-Boc-N*ε*-*Z*-Lys-OH, HBTU, HOBt, DIPEA, DMF, room temp; (f) H_2, 10% Pd/C, MeOH, room temp.

Scheme 4. Synthesis of Molecular Tongs 1 and 3[a]

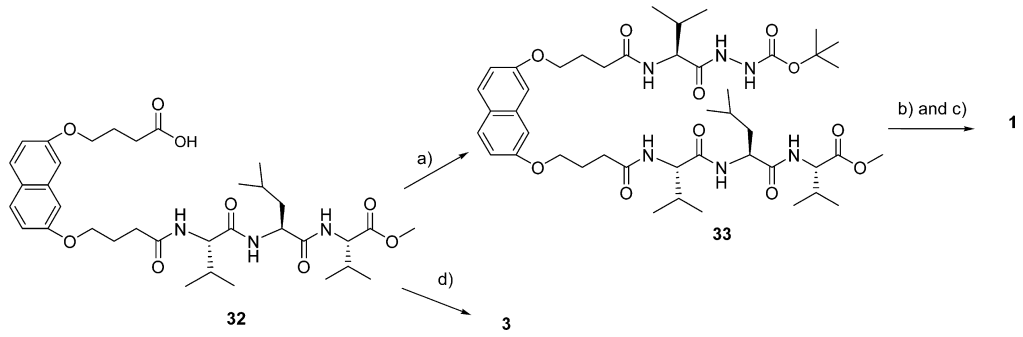

[a](a) **12**, HBTU, DIPEA, DMF, 5 days, room temp; (b) HCl/EtOH, DMF, room temp; (c) *N*-Boc-Val-OH, HBTU, Et_3N, DMF, room temp; (d) **19**, HBTU, HOBt, DIPEA, room temp.

butyryl-Val-Leu-Val-OMe **32**,[21] with the peptidomimetic **19** in satisfactory yield (49%) (Scheme 4).

Molecular tongs **2** was synthesized from 4-((7-(3-carboxypropoxy)-2-naphthyl)oxy)butanoic acid **34**[20] by a standard coupling protocol (using HBTU and HOBt) to peptidomimetics **14** in 39% yield (Scheme 5). Molecule **10**, which has only one peptidomimetic arm, was obtained as a byproduct, resulting from incomplete coupling, in 9% yield. The molecular tongs **4**–**9** were synthesized from 4-((7-(3-carboxypropoxy)-2-naphthyl)oxy)butanoic acid **34**[20] by a standard coupling protocol (using HBTU and HOBt) to peptidomimetics **19**, **21**, **23**, **27**, **29**, and **31**, respectively, in satisfactory yields (40–73%) (Scheme 5).

Scheme 5. Synthesis of Molecular Tongs 2 and 4–10[a]

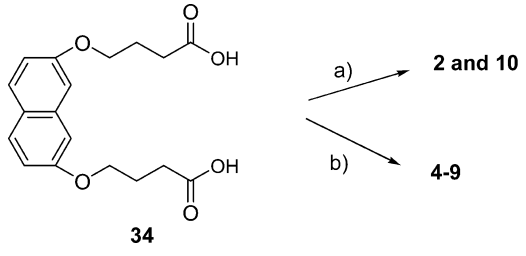

[a](a) HBTU, HOBt, DIPEA, **14**, DMF, room temp; (b) HBTU, HOBt, DIPEA, **19** or **21** or **23** or **27** or **29** or **31**, DMF, room temp.

RESULTS AND DISCUSSION

We used a fluorimetric assay to test the capacity of compounds **1**–**10** to inhibit recombinant wild-type PR (PR) at the optimum pH (4.7) and 30 °C.[18,20–22] Compounds **5**, **8**, and **9** were not inhibitors at the highest tested concentration of 28 μM, whereas compounds **6** and **7** inhibited the enzyme poorly (13 and 21% at 28 μM, respectively). In contrast, compounds **1**–**4** efficiently inhibited both PR and the two multimutated proteases, MDR-HM and ANAM-11. The mutant MDR-HM[30] contains six amino acid mutations located within and outside the active site of the enzyme (Leu10Ile/Met46Ile/Ile54Val/Val82Ala/Ile84Val/Leu90Met), while ANAM-11[31] has 11 mutations: (Leu10Ile/Met36Ile/Ser37Asp/Met46Ile/Arg57Lys/Leu63Pro/Ala71Val/Gly73Ser/Ile84Val/Leu90-Met/Ile93Leu).

We used Zhang–Poorman kinetic analysis to identify the mechanism of inhibition. Plots of $[E]_0/\sqrt{vi}$ versus $\sqrt{vi}$ were constructed, where vi were the initial rates. In all cases, parallel lines were obtained, in agreement with dimerization inhibition (Figure 4). The corresponding inhibition constants K_{id} are

dx.doi.org/10.1021/jm300181j | J. Med. Chem. 2012, 55, 6762–6775

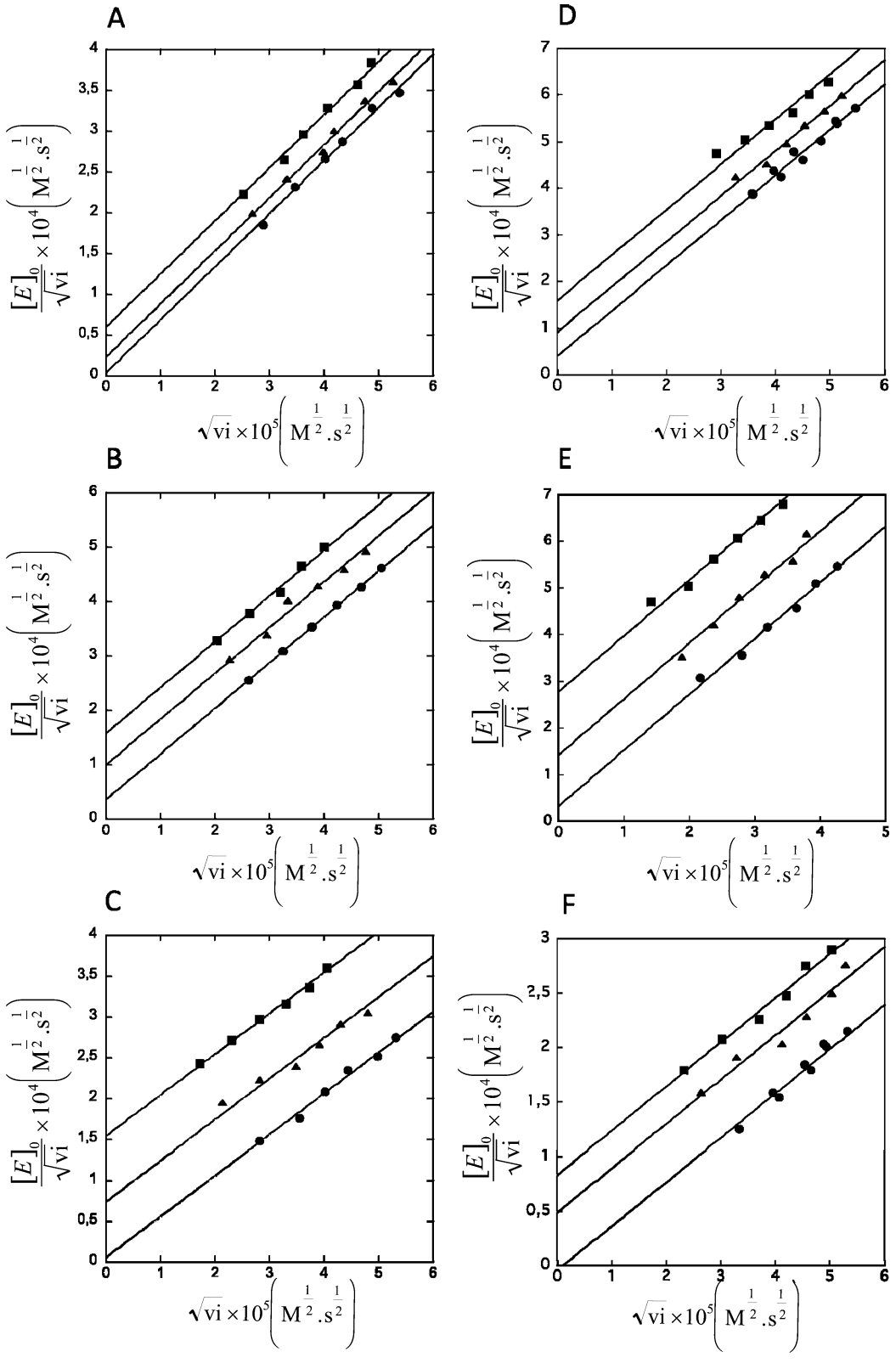

Figure 4. (A–C) Zhang kinetic analyses of PR, MDR-HM, and ANAM-11 inhibition by compounds **2** and **4** at pH 4.7 and 30 °C. (A) PR inhibition by 2.8 μM **2** (■), 2 μM **2** (▲); (B) MDR-HM inhibition by 2.8 μM **2** (■) and 1.9 μM **2** (▲); (C) ANAM-11 by 4.2 μM **2** (■) and 2.8 μM **2** (▲); (D) PR inhibition by 17 μM **4** (■), 11 μM **4** (▲); (E) MDR-HM inhibition by 8.5 μM **4** (■) and 5.6 μM **4** (▲); (F) ANAM-11 by 22 μM **4** (■) and 17 μM **4** (▲). Enzyme activity was also always measured without inhibitor (●).

shown in Table 1. The mechanism of inhibition was confirmed for the four compounds using fluorescent probe binding. The hydrophobic 1-anilino-8-naphthalene sulfonate (ANS) is preferentially bound to the hydrophobic surfaces of proteins.[32] We observed important enhancements of the fluorescence due to ANS when compounds **1**–**3** and **P1** were added to the

dx.doi.org/10.1021/jm300181j | J. Med. Chem. 2012, 55, 6762–6775

Table 1. Inhibition of PR and Mutated HIV-1 Proteases MDR-HM and ANAM-11 by Compounds 1−10 (30 °C and pH 4.7)[a]

compd	clogP	hydrophobic surface (Å^2)	hydrophilic surface (Å^2)	K_{id} (nM) PR	MDR-HM	ANAM-11
P1	7.8	1467	232	560[20]	nd	nd
1	8.5	1443	281	90	160	100
2	9.3	1391	326	50	160	80
3	4.0	1079	398	150	270	170
4	0.1	673	555	700	1600	800

compd	clogP	hydrophobic surface (Å^2)	hydrophilic surface (Å^2)	% inhibition at 28 μM
5	3.2	797	570	0
6	1.4	639	465	13
7	3.4	911	468	21
8	2.1	794	548	0
9	5.6	1304	595	0
10	6.4	924	270	0

[a]Standard errors of initial rates are less than 5%. clogP and solvent accessible surface areas are indicated. nd: not determined.

enzyme (less marked for **4**) (Figure 5) but not when the active-site inhibitors acetylpepstatin, saquinavir, or amprenavir were

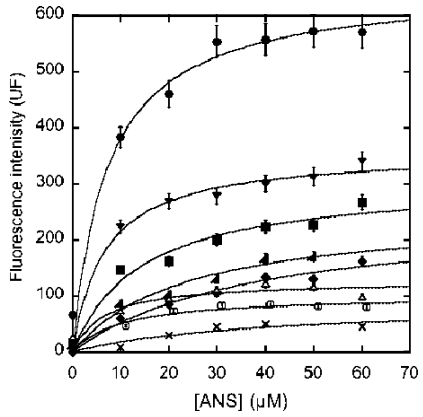

Figure 5. ANS emission fluorescence (470 nm) measured at pH 4.7 and 25 °C. The excitation wavelength was 370 nm. PR (275 nM) was preincubated in the absence of inhibitor (△) or in the presence of acetylpepstatin (×), saquinavir (○), and compounds **1** (■), **2** (●), **3** (▲), **4** (◆), and **P1** (▼) prior to adding ANS. The final DMSO concentration was always 0.2% (v/v). Fluorescence intensity was corrected for the fluorescence of the same concentrations of ANS and inhibitor without enzyme.

added. Inhibitors **1**−**4** and the parent peptidic molecule **P1** were bound to the unmasked hydrophobic surfaces of PR. This is in agreement with the expected exposure of hydrophobic interface area when the dimer is destabilized or dissociated.[14,15] In contrast, active-site inhibitors changed the conformation from semiclosed (dimer alone) to closed (active-site inhibitor/dimer complex),[15] leading to a smaller decrease in the ANS fluorescence than that observed with the PR alone. The experimental results summarized in Table 1 indicate that the introduction of pseudopeptidic arms containing two Val residues linked by an hydrazine bridge dramatically increased the inhibitory potency (K_{id}s of 90 nM for **1** and 50 nM for **2**) over those previously reported for the peptidic arm Val-Leu-Val (**P1**, 560 nM)[20] and to the Val-(5-acetamido-2-methoxybenzo-hydrazide) arm (∼200 nM).[22] They also show that the one-arm molecule **10** is not an inhibitor, in agreement with our previous results showing that there must be two peptide strands on the molecular tongs to inhibit dimerization.[20] Third, inhibition was not affected by inserting an azatide moiety (diazaglycine) into one arm directly linked to the carboxypropyloxy group while the other arm was a tripeptide (Val-Leu-Val) (K_{id} of 150 nM for **3** and 90 nM for **1**). However, inhibitory activity was decreased when azatide moieties were introduced in both arms and directly linked to the carboxypropyloxy group (K_{id} of 700 nM for **4** and 50 nM for **2**). Inserting an azatide moiety at the *C*-terminus via a Val residue made the symmetric molecule **7** almost completely devoid of inhibitory activity (21% inhibition at 28 μM). Similarly, further increasing the flexibility by introducing a β-Ala residue or a Lys residue linked through its ε-amino group completely suppressed inhibitory activity (**8** and **9** relative to **4**). The increased flexibility at the *N*-termini destroyed all inhibitory activity in contrast to our previous observation with 5-acetamido-2-methoxybenzohydrazide and 3-amino-6-methylpyridine(1*H*)-one strands.[22,23] The azatide peptidomimetic unit is thus best directly attached to the carboxypropyloxy linker (**3**, **4**). Lastly, shortening both arms by removing the *C*-terminal valinamide gave the poorly active compound **6**. Lengthening both arms with a β-Ala residue linked to the *C*-terminal side (compound **5**) gave a poorer inhibitor. These two last observations are in accordance with our previous results showing that a tripeptide sequence is better than the shorter dipeptide or longer tetrapeptide sequences.[20,21] The decreased inhibitory activity of molecular tongs **5** and **6** can be also ascribed to the lack of hydrophobic valine side chain, while compound **4** has valine residues. We used molecular modeling to estimate three physical properties of the molecules, clogP, hydrophobic surface area, and hydrophilic surface area (Table 1), in order to further correlate the inhibitory activity with the hydropathic properties of the molecules. A favorable influence of hydrophobicity on inhibitory activity was observed as previously reported for some molecular tongs.[21,23]

The presence in the molecular tongs arms of carbonylhydrazide (CONHNHCO) peptidomimetic fragments that have particular hydrogen bonding properties led to a noticeable increase of the inhibitory activity for compounds **1** and **2** compared to **P1** (factors of 6.2 and 11.2 against PR), whereas clogP was poorly increased (factors of 1.08 and 1.19, respectively). Both inhibitory activity and cLogP were improved for compound **3** (factor of 3.7 for PR inhibition and 1.95 for cLogP). For the most soluble compound, **4** (≈ 0.3 mg/mL), the inhibitory activity was only decreased by a factor of 1.25 whereas cLogP was improved by a factor of 78. These data show that both activity and solubility can be increased (compound **3**). An important decrease of cLogP (factor of 78) and hydrophobic surface (factor of 2.17) and increase in hydrophilic surface (2.39) did not comprise the inhibitory efficiency (compound **4**). These data highlight the difficulty but the possibility to find a compromise between hydrophilicity and inhibitory activity.

Remarkably, the four new molecular tongs **1**−**4** behaved as antidimers against the two multimutated proteases ANAM-11 and MDR-HM, which are analogous to the proteases found in multiresistant viruses (Table 1). The inhibition of the two mutated proteases by compounds **1**−**3** remained essentially identical for a given mutated protease (for example, K_{id} of **2**: 120 nM for MDR-HM and 80 nM for ANAM-11). Compound

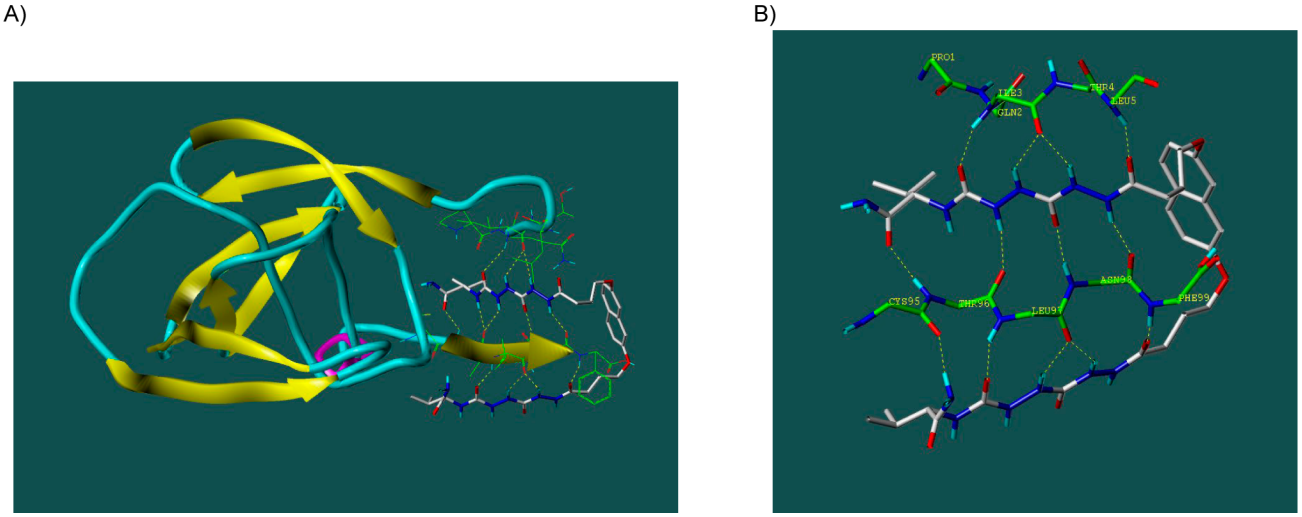

Figure 6. Putative complexes between PR monomer and the peptidomimetic molecular tong **4** (color by atom type): (A) one PR-monomer (ribbon tube representation); (B) the *C*- and *N*-termini of one PR-monomer (green backbone).

4 was the poorest inhibitor of both PR and the mutated proteases (Table 1).

We used molecular modeling to build several complexes that might be formed between our new molecular tongs **1**–**9** and the PR monomer and used them to correlate inhibitory activity with structural characteristics. We used one monomer from the crystallographic data for the dimeric PR and built molecular tongs using the *C*- and *N*-terminal ends of the removed second monomer of PR as templates. The designed carbonylhydrazide peptidomimetics had an extended conformation compatible with the formation of a β-sheet. The energy of the monomer–molecular tongs complexes was minimized. This minimization did not disrupt the postulated β-sheet structure formed between the *N*- and *C*-termini of the remaining PR monomer and molecular tongs **1**–**6**. The carbonylhydrazide peptidomimetic arms still had an extended conformation. The PR–molecular tongs complexes had an extensive network of hydrogen bonds. The correct array of alternating 10-member and 14-member rings involving two consecutive hydrogen bonds was maintained after minimization (see Figure 6 and Supporting Information). For example, there were still 13 hydrogen bonds in the complex with molecular tongs **4** (Figure 6). Most of them were with the *C*-terminal end (nine for molecular tongs **4** and only five with the *N*-terminal end). Conversely, there was no stable β-sheet structure with molecular tongs **7**–**9** after minimization (see Supporting Information). The biological results are in agreement with the proposed complexes designed by molecular modeling; molecules **1**–**4** interacted more strongly with the monomer than did molecules **7**–**9**. The absence of inhibitory activity of **5** and **6** compared to **4** may be explained by the lack of hydrophobic amino acid side chains in **5** and **6** because hydrophobic interactions are beneficial for stabilizing β-sheet structures. Valine side chain(s) may reinforce the binding of molecular tongs to the monomer ends and explain the improved inhibitory efficiency of molecular tongs **1**–**4**. The same holds if we compare compound **4** (only one valine side chain per arm) with compound **1** (two valine and one leucine side chains in one arm, and two valine side chains in the other) and with compound **2** (two valine side chains per arm). We observed that the number of hydrogen bonds formed with the inhibitor and the *N*- and *C*-termini of the remaining PR monomer was higher for **4** than for **1** and **2** (13 against eight and nine for compounds **1** and **2**, respectively). However, as indicated above, hydrophobic interactions are missing for compound **4** to further stabilize the β-sheet structure.

Finally, we determined the stability of the symmetrical molecular tongs **2** and **4** and asymmetrical molecular tongs **1** and **3** in RPMI culture medium containing 20% fetal calf serum (Figure 4S in Supporting Information). The half-lives of compounds **1** and **3** were about 24 h, which is very similar to the 28 h half-life of the **P1** peptide molecular tong bearing Val-Leu-Val[21] (Figure 1). Conversely, compounds **2** and **4** were not significantly degraded after incubation for 48 h. These results suggest that they are more resistant to hydrolysis than the previously described peptide molecules and about the same as those with 5-acetamido-2-methoxybenzohydrazide peptidomimetics (no significant degradation after 33 h).[22] The metabolic stability of the molecular tongs with two peptidomimetic arms was also better than that of the asymmetrical molecules bearing one tripeptidic arm.

Last, we evaluated the selectivity of molecules **1**–**4** toward two other aspartic proteases, monomeric renin and pepsin. Neither renin nor pepsin was inhibited by 10 μM concentrations of compounds **1**–**4**.

CONCLUSION

We have designed and synthesized a new series of naphthalene-based molecular tongs containing carbonylhydrazide (CONHNHCO) and oligohydrazide (azatide) peptidomimetic side arms. Their original hydrogen bonding properties made these peptidomimetics good modulators of protein–protein interactions involving β-sheet structures. Their scaffold gave the molecular tongs some rigidity and forced the arms of the tongs to have the extended structure essential for mimicking a β-strand. As a proof-of-concept, we tested the ability of these molecules to disrupt the PR termini β-sheet interface in order to inhibit PR. The best of our nonpeptide molecular tongs inhibited PR dimerization with an inhibition constant K_{id} of 50 nM, which is the best inhibition of HIV-1 PR dimerization reported to date for molecular tongs. The azatide-based scaffolds also increased water solubility. However, the inhibitory potencies varied greatly according to the molecule structures, indicating that there must be appropriate balances between

dx.doi.org/10.1021/jm300181j | J. Med. Chem. 2012, 55, 6762–6775

rigidity and flexibility, and between hydrophilicity and hydrophobicity, in order to obtain powerful inhibitors. The example of the inhibitor **4** shows that water solubility does not compromise inhibitory efficiency. The ability of these proteolysis-resistant molecules to inhibit the multimutated ANAM-11 highlights their potential to successfully overcome the resistance to classical PI protease inhibitors presently encountered.

EXPERIMENTAL SECTION

Chemistry. All solvents were purchased from commercial sources. Dimethylformamide (DMF) was distilled over $CaSO_4$, tetrahydrofuran (THF) was distilled over sodium/benzophenone, and acetonitrile was distilled over $CaCl_2$. TLC was performed on 60F-250 silica gel (0.26 mm thick plates. Spots were visualized with UV light (254 nm), 3.5% phosphomolybdic acid in ethanol, or with a solution of ninhydrin in ethanol. Liquid chromatography was performed on Merck 60 silica gels (230−400 mesh). Protected amino acids, *O*-benzotriazol-1-yl-*N*,*N*,*N*′,*N*′-tetramethyluronium hexafluorophosphate (HBTU), and 1-hydroxybenzotriazol (HOBT) were purchased from commercial sources. 4-[7-(3-Carboxy-propoxy)naphthalene-2-yloxy]butyryl-Val-Leu-Val-OMe **32**[21] and 4-((7-(3-carboxypropoxy)-2-naphthyl)oxy)-butanoic acid **34**,[20] were prepared according to published methods. Melting points were determined on a Kofler melting point apparatus. NMR spectra were obtained on Ultrafield AVANCE 300 (^{1}H, 300 MHz ; ^{13}C, 75 MHz) or Bruker AVANCE 400 (^{1}H, 400 MHz; ^{13}C, 100 MHz) spectrometers. $CDCl_3$ was used as solvent unless otherwise stated. Chemical shifts (δ) are in ppm, and the following abbreviations are used: singlet (s), doublet (d), doublet doublet (dd), triplet (t), quadruplet (q), multiplet (m), doublet triplet (dt), and broad singlet (bs). Mass spectra (APCI and ESI) were obtained using a Bruker Esquire-LC apparatus at the SAMM (Faculty of Pharmacy at Châtenay-Malabry). Elemental analyses (C, H, N) were performed on a Perkin-Elmer CHN Analyzer 2400 at the Microanalyses Service of the Faculty of Pharmacy at Châtenay-Malabry (France). Elemental analysis data are included in the Supporting Information. The purity of molecular tongs was determined by HPLC using a WATERS modular system (quaternary pump + controller E600, UV detector PDA 2996, autosampler 717). All molecular tongs tested in biological assays were 95% pure. HPLC conditions were as follows. Method 1: column SUNFIRE, C18, 5 μm, 150 mm × 4.6 mm; mobile phase, a mixture of (A) water (0.05% TFA) and (B) AcCN (0.05% TFA); room temperature; flow rate 1 mL/min; detection at 254 nm. Method 2: column SUNFIRE, C18, 5 μm, 150 mm × 4.6 mm; mobile phase a mixture of (A) water (0.05% TFA) and (B) MeOH (0.05% TFA); room temperature; flow rate 1 mL/min; detection at 235 nm.

*Synthesis of Molecular Tongs (**1**).* Product **33** (80 mg, 92 μmol, 1 equiv) was dissolved in DMF (4 mL), and 2 mL of 9 M HCl in ethanol was added and the mixture stirred for 4 h. Then, Et_3N (35 μL, 248 μmol, 2.7 equiv), HBTU (42 mg, 110 μmol, 1.2 equiv), and *N*-Boc-Val-OH (20 mg, 91.8 μmol, 1 equiv) were added and the mixture stirred again at room temperature for 5 days. The DMF was removed under reduced pressure, and CH_2Cl_2 was added to the crude product to precipitate a solid, which was washed successively with CH_2Cl_2, aqueous 0.1 M HCl, aqueous 10% $NaHCO_3$, brine, and again with CH_2Cl_2 to yield **1** (49 mg, 55%) as a light-brown solid; mp 213-216 °C. ^{1}H NMR (300 MHz, DMSO-d_6): δ 9.92 (s, 1H), 9.82 (s, 1H), 9.69 (s, 1H), 8.72 (s, 1H), 7.91−8.01 (m, 3H), 7.71 (d, J = 8.7 Hz, 2H), 7.17 (s, 2H), 6.97 (d, J = 8.7 Hz, 2H), 4.35−4.43 (m, 1H), 4.12−4.24 (m, 4H), 4.06 (t, J = 6.6 Hz, 4H), 3.61 (s, 3H), 2.33−2.43 (m, 4H), 1.90−2.06 (m, 8H), 1.54−1.66 (m, 1H), 1.44−1.49 (m, 2H), 1.38 (s, 9 H), 0.77−0.96 (m, 30 H). ^{13}C NMR (75 MHz, DMSO-d_6): δ 172.1, 171.6, 171.4, 170.8, 170.1, 169.8, 156.9, 155.2, 135.6, 128.8, 123.6, 115.8, 106.0, 78.9, 66.8, 57.7, 57.2, 55.9, 51.5, 50.7, 40.6, 31.5, 31.4, 30.5, 30.1, 29.7, 27.9, 24.9, 24.9, 24.0, 22.8, 21.5, 19.1, 19.0, 18.7, 18.2, 18.1, 18.0. APCI$^+$ MS m/z 970 [M + H]$^+$. IR (neat): ν_{max} 3277, 2963, 1743, 1633, 1537, 1386, 1209, 1163, 1021, 831, 668 cm^{-1}. HPLC purity: method 1, mixture A/B from 60/40 to 0/100 in 20 min, TR = 14.1 min, 97.5%; method 2, mixture A/B from 40/60 to 0/100 in 30 min, TR = 24.1 min, 97%. Anal. ($C_{50}H_{79}N_7O_{12}\cdot 6H_2O$) C, H, N.

*Synthesis of Molecular Tongs (**2**) and Molecule (**10**).* Compound **14** (327 mg, 0.99 mmol, 2.2 equiv) was dissolved in DMF (5 mL) at 0 °C was mixed with compound **34** (150 mg, 0.45 mmol, 1 equiv), DIPEA (145 mg, 0.99 mmol, 2.2 equiv), HOBt (134 mg, 0.99 mmol, 2 equiv), and HBTU (426 mg, 0.99 mmol, 2.2 equiv), and the mixture was stirred for 48 h at room temperature. DMF was removed under reduced pressure, and the resulting solid was washed successively with CH_2Cl_2 (5 mL), 10% aqueous 10% citric acid (10 mL), water (10 mL), 10% aqueous K_2CO_3 (10 mL), and again with CH_2Cl_2 (5 mL). Purification by HPLC gave products **2** (168 mg, 39%) and **10** (26 mg, 9%) as white solids. Product **2**: mp 220−223 °C. ^{1}H NMR (400 MHz, DMSO-d_6): δ 9.92 (s, 2H), 9.82 (s, 2H), 7.97 (d, J = 8.1 Hz, 2H), 7.70 (d, J = 8.6 Hz, 2H), 7.18 (s, 2H), 6.97 (d, J = 8.8 Hz, 2H), 6.66 (d, J = 8.2 Hz, 2H), 4.22 (t, J = 8.1 Hz, 2H), 4.06 (t, J = 6.4 Hz, 4H), 3.81 (t, J = 8.2 Hz, 2H), 2.37 (q, J = 6.9 Hz, 4H), 1.99 (t, J = 6.9 Hz, 4H), 1.94 (m, 2H), 1.90 (m, 2H), 1.37 (s, 18H), 0.92 (d, J = 6.5 Hz, 12H), 0.86 (d, J = 6.2 Hz, 12H). ^{13}C NMR (100 MHz, DMSO-d_6): δ 171.6, 170.2, 169.9, 157.0, 155.3, 135.7, 128.9, 123.7, 115.9, 106.1, 77.9, 67.0, 58.2, 56.1, 31.5, 30.6, 30.5, 28.2, 25.0, 19.1, 18.3. IR (neat): ν_{max} 3221, 2036, 1605, 1478, 1209, 1169, 829, 651 cm^{-1}. ESI$^+$ MS m/z 979 [M + Na]$^+$. HPLC purity: method 1, mixture A/B from 60/40 to 0/100 in 20 min, TR = 11.5 min, 96%; method 2, mixture A/B from 40/60 to 0/100 in 20 min, TR = 19.9 min, 99%. Anal. ($C_{48}H_{76}N_8O_{12}\cdot 5H_2O$) C, H, N. Product **10**: mp °C. ^{1}H NMR (400 MHz, DMSO-d_6): δ 11.90 (bs, 1H), 9.95 (s, 1H), 9.79 (s, 1H), 7.98 (d, J = 8.1 Hz, 1H), 7.70 (d, J = 8.6 Hz, 2H), 7.20 (s, 2H), 6.97 (d, J = 8.8 Hz, 2H), 6.68 (d, J = 8.2 Hz, 1H), 4.25 (t, J = 8.1 Hz, 1H), 4.08 (t, J = 6.4 Hz, 4H), 3.81 (t, J = 8.2 Hz, 1H), 2.40 (m, 4H), 1.97 (m, 6H), 1.37 (s, 9H), 0.91 (d, J = 6.5 Hz, 6H), 0.86 (d, J = 6.2 Hz, 6H). ^{13}C NMR (100 MHz, DMSO-d_6): δ 171.6, 170.2, 169.9, 157.0, 155.3, 135.7, 128.9, 123.7, 115.9, 106.1, 77.9, 66.9, 66.5, 58.1, 56.1, 31.5, 30.5, 30.1, 28.1, 24.9, 24.2, 19.1, 18.3. IR (neat): ν_{max} 3221, 2036, 1605, 1478, 1209, 1169, 827, 652 cm^{-1}. ESI$^-$ MS m/z 643 [M − H]$^-$. HPLC purity: method 1, mixture A/B from 60/40 to 0/100 in 20 min, TR = 8.5 min, 100%. Anal. ($C_{33}H_{48}N_4O_9$) C, H, N.

*Synthesis of Molecular Tongs (**3**).* Compounds **19** (88 mg, 0.38 mmol) and **32** (230 mg, 0.35 mmol) were dissolved in DMF, to which were added DIPEA (207 μL, 1.2 mmol, 3.5 equiv), HBTU (159 mg, 0.42 mmol, 1.2 equiv), and HOBt (52 mg, 0.38 mmol, 1.1 equiv), and the mixture was stirred for 24 h at room temperature under an argon atmosphere. The solvent was removed under reduced pressure to give a beige oil. Trituration in EtOAc yielded a beige solid that was collected on a filter and washed successively with EtOAc, CH_2Cl_2, H_2O, CH_3OH, and Et_2O to give **3** as a white powder (150 mg, 49%); mp 218−220 °C. ^{1}H NMR (400 MHz, DMSO-d_6): δ 9.63 (s, 1H), 8.20 (br s, 2H), 7.92−7.97 (m, 3H), 7.78 (s, 1H), 7.71 (d, J = 9.3 Hz, 2H), 7.32 (bs, 1H), 7.17 (s, 2H), 7.05 (s, 1H), 6.98 (bs, 2H), 6.09 (d, J = 7.2 Hz, 1H), 4.36−4.40 (m, 1H), 3.99−4.17 (m, 7H), 3.60 (s, 3H), 2.33−2.37 (m, 4H), 1.98−2.03 (m, 7H), 1.60 (bs, 1H), 1.44 (bs, 2H), 0.81−0.85 (m, 24H). ^{13}C NMR (100 MHz, DMSO-d_6): δ 173.5, 172.2, 171.7, 170.9, 158.3, 158.1, 157.0, 135.7, 129.0, 123.7, 115.9, 106.2, 66.9, 66.8, 57.8, 57.6, 57.3, 51.6, 50.8, 40.8, 31.6, 30.7, 30.3, 29.9, 29.7, 25.1, 24.4, 24.1, 23.0, 21.6, 19.3, 19.2, 18.8, 18.2, 18.1, 17.4. IR (neat): ν_{max} 3278, 2963, 1632, 1545, 1210 cm^{-1}. ESI$^+$ MS m/z 895 [M + Na]$^+$, 911 [M + 39]$^+$. HPLC purity: method 1, mixture A/B from 60/40 to 0/100 in 20 min, TR = 8.1 min, 96%; method 2, mixture A/B from 40/60 to 0/100 in 30 min, TR = 24.1 min, 97%. Anal. ($C_{42}H_{65}N_9O_{11}\cdot 1.5H_2O$) C, H, N.

*Synthesis of Molecular Tongs (**4**).* Same procedure as for **3** from **34** and **19**. Product **4** was obtained as a white powder (174 mg, 56%); mp 181−185 °C. ^{1}H NMR (400 MHz, DMSO-d_6) δ 9.63 (s, 2H), 8.20 (bs, 4H), 7.77 (s, 2H), 7.71 (d, J = 8.8 Hz, 2H), 7.32 (bs, 2H), 7.18 (s, 2H), 7.05 (s, 2H), 6.97 (d, J = 7.6 Hz, 2H), 6.08 (d, J = 8.4 Hz, 2H), 3.97−4.08 (m, 6H), 2.31−2.34 (m, 4H), 1.91−2.03 (m, 6H), 0.85 (d, J = 6.7 Hz, 6H), 0.82 (d, J = 6.7 Hz, 6H). ^{13}C NMR (100 MHz, DMSO-d_6): δ 173.5, 171.8, 158.3, 158.1, 157.0, 135.7, 129.0, 123.7, 115.9, 106.2, 66.7, 57.6, 30.7, 29.6, 24.4, 19.3, 17.4. IR (neat): ν_{max} 3252, 2967, 1657, 1516, 1211 cm^{-1}. ESI$^+$ MS m/z 783 [M + Na]$^+$, 799 [M +

dx.doi.org/10.1021/jm300181j | J. Med. Chem. 2012, 55, 6762−6775

K]$^+$. HPLC purity: method 1, mixture A/B from 70/30 to 0/100 in 20 min, TR = 3.4 min, 100%; method 2, mixture A/B from 70/30 to 0/100 in 20 min, TR = 15.6 min, 97%. Anal. ($C_{32}H_{48}N_{12}O_{10}\cdot1.5H_2O$) C, H, N.

*Synthesis of Molecular Tongs (**5**).* Same procedure as for **3** from **34** and **21**. Product **5** was obtained as a pale-gray powder (174 mg, 73%); mp 177−187 °C. ^{1}H NMR (400 MHz, DMSO-d_6): δ 9.60 (s, 2H), 8.14 (bs, 4H), 7.70−7.72 (m, 4H), 7.19 (s, 2H), 6.97 (d, J = 8.4 Hz, 2H), 6.23 (br, 2H), 4.08 (br, 4H), 2.59 (s, 6H), 3.22−3.28 (m, 4H), 2.43−2.47 (m, 4H), 2.32 (t, J = 7.1 Hz, 4H), 2.02 (br, 4H). ^{13}C NMR (100 MHz, DMSO-d_6): δ 171.9, 158.5, 158.1, 157.0, 135.7, 129.0, 123.7, 115.9, 106.2, 66.8, 51.3, 35.3, 34.3, 29.7, 24.5. IR (neat): ν_{max} 3304, 2947, 1663, 1552, 1208 cm^{-1}. ESI$^+$ MS m/z 757 [M + Na]$^+$. HPLC purity: method 1, mixture A/B from 70/30 to 0/100 in 20 min, TR = 4.1 min, 100%. Anal. ($C_{30}H_{42}N_{10}O_{12}\cdot2H_2O$) C, H, N.

*Synthesis of Molecular Tongs (**6**).* Same procedure as for **3** from **34** and **23**. Product **6** was obtained as a white powder (98 mg, 55%); mp 206−210 °C. ^{1}H NMR (400 MHz, DMSO-d_6): δ 9.59 (s, 2H), 8.14 (bs, 4H), 7.63−7.72 (m, 4H), 7.19 (s, 2H), 6.96 (s, 2H), 6.09 (br, 2H), 4.08 (br, 4H), 2.57 (s, 6H), 2.33−2.42 (m, 4H), 2.01 (br, 4H). ^{13}C NMR (100 MHz, DMSO-d_6): δ 174.1, 159.2, 158.1, 156.9, 135.7, 128.9, 123.7, 115.9, 106.1, 66.6, 29.7, 26.2, 24.2. IR (neat): ν_{max} 3280, 2947, 1664, 1515, 1210 cm^{-1}. ESI$^+$ MS m/z 613 [M + Na]$^+$. HPLC purity: method 1, mixture A/B from 80/20 to 0/100 in 30 min, TR = 11.7 min, 98%; method 2, mixture A/B from 40/60 to 0/100 in 30 min, TR = 24.1 min, 97%. Anal. ($C_{24}H_{34}N_{10}O_8\cdot2H_2O$) C, H, N.

*Synthesis of Molecular Tongs (**7**).* Same procedure as for **3** from **34** and **27.** Product **7** was obtained as a brown solid (140 mg, 69%); mp 208−210 °C. ^{1}H NMR (400 MHz, DMSO-d_6): δ 9.70 (s, 2H), 9.49 (s, 2H), 8.30 (s, 2H), 8.04 (s, 2H), 7.97 (d, J = 8.3 Hz, 2H), 7.70 (d, J = 8.9 Hz, 2H), 7.18 (s, 2H), 6.97 (dd, J = 8.8, 1.8 Hz, 2H), 4.20−4.15 (m, 2H), 4.08−4.04 (m, 4H), 2.38 (m, 4H), 2.00−1.97 (m, 6H), 1.80 (s, 6H), 0.90−0.85 (m, 12H). ^{13}C NMR (100 MHz, DMSO-d_6): δ 171.8, 170.8, 168.9, 157.2, 156.9, 135.7, 128.9, 123.6, 115.9, 106.0, 66.9, 56.3, 31.4, 30.4, 24.9, 20.5, 19.0, 18.3. IR (neat): ν_{max} 3275, 1630, 1514, 1209 cm^{-1}. APCI $^+$ MS m/z 782 [M + Na]$^+$. HPLC purity: method 1, mixture A/B 60/40, TR = 4.1 min, 96%; Method 2, mixture A/B from 50/50 to 20/80 in 20 min, TR = 5.88 min, 95%. Anal. ($C_{34}H_{50}N_{10}O_{10}\cdot0.75H_2O$), C, H, N.

*Synthesis of Molecular Tongs (**8**).* Same procedure as for **3** from **34** and **29**. Product **8** was obtained as a light-brown solid (53 mg, 40%); mp 225−227 °C. ^{1}H NMR (400 MHz, DMSO-d_6): δ 9.53 (bs, 4H), 8.24 (bs, 4H), 7.90 (bs, 2H), 7.70 (d, J = 8.9 Hz, 2H), 7.18 (s, 2H), 6.96 (dd, J = 8.9, 2 Hz, 2H), 4.05 (m, 4H), 3.27 (m, 4H), 2.27 (m, 8H), 2.00 (m, 4H), 1.80 (s, 6H). ^{13}C NMR (100 MHz, DMSO-d_6): δ 171.6, 170.2, 168.8, 157.5, 157.0, 135.8, 128.9, 123.7, 115.9, 106.1, 66.9, 35.1, 33.5, 31.7, 24.8, 20.6. IR (neat): ν_{max} 3277, 2967, 1629, 1514, 1160 cm^{-1}. ESI$^+$ MS m/z 725 [M + Na]$^+$, 741 [M + K]$^+$]$^+$. HPLC purity: method 1, mixture A/B from 90/10 to 0/100, TR = 10.8 min, 100%; method 2, mixture A/B from 70/30 to 0/100 in 20 min, TR = 13 min, 100%. Anal. ($C_{30}H_{42}N_{10}O_{10}\cdot3H_2O$) C, H, N.

*Synthesis of Molecular Tongs (**9**).* Same procedure as for **3** from **34** and **31**. Product **9** was obtained as a light-yellow solid (120 mg, 60%); mp 157−159 °C. ^{1}H NMR (300 MHz, CD_3OD): δ 7.63 (d, J = 9 Hz, 2H), 7.12 (s, 2H), 6.94 (dd, J = 8.8, 2.1 Hz, 2H), 4.10 (m, 4H), 3.98 (t, J = 7.1 Hz, 2H), 3.19 (m, 4H), 2.42 (t, J = 7.3 Hz, 4H), 2.13 (m, 4H), 1.97 (s, 6H), 1.75 (m, 2H), 1.64 (m, 2H), 1.51 (m, 4H), 1.43 (s, 18H), 1.42 (m, 4H). ^{13}C NMR (75 MHz, CD_3OD): δ 175.6, 175.0, 173.1, 159.9, 158.8, 158.1, 137.5, 130.0, 125.8, 117.2, 107.3, 80.9, 68.2, 54.9, 40.1, 33.7, 32.4, 30.0, 28.7, 26.7, 24.0, 20.5. IR (neat): ν_{max} 3215, 1642, 1542, 1212 cm^{-1}. ESI$^+$ MS m/z 1040 [M + Na]$^+$]$^+$. HPLC purity: method 1, mixture A/B from 70/30 to 0/100, TR = 9.2 min, 100%; method 2, mixture A/B from 50/50 to 0/100 in 30 min, TR = 19.5 min, 100%. Anal. ($C_{46}H_{72}N_{12}O_{14}\cdot4H_2O$) C, H, N.

*tert-Butyl N-[[(2S)-2-(Benzyloxycarbonylamino)-3-methyl-butanoyl]amino]carbamate (**11**).* *N*-*Z*-Val-OH (2 g, 7.97 mmol, 1 equiv) was dissolved in CH_2Cl_2 (30 mL) at 0 °C and to it were added successively, DIPEA (3.1 g, 23.9 mmol, 3 equiv), *tert*-butyl carbazate (1.16 g, 8.77 mmol, 1.1 equiv), HOBt (1.19 g, 8.77 mmol, 1.1 equiv), and EDCI (1.68 g, 8.77 mmol, 1.1 equiv). This mixture was stirred overnight at room temperature and then diluted with EtOAc (50 mL). The organic phase was washed with 10% aqueous citric acid (5 mL), water (10 mL), 10% aqueous K_2CO_3 (5 mL), and brine (5 mL). It was then dried over $MgSO_4$, filtered, and concentrated under reduced pressure to give **11** as a white powder (2.5 g, 88%); mp 141−143 °C. ^{1}H NMR (300 MHz, CD_3OD): δ 7.43 (m, 5H), 5.12 (s, 2H), 4.08 (m, 1H), 2.10 (m, 1H), 1.47 (s, 9H), 1.03 (d, J = 7.0 Hz, 3H), 0.99 (d, J = 7.0 Hz, 3H). ^{13}C NMR (75 MHz, CD_3OD): δ = 173.7, 158.5, 157.4, 138.2, 129.6, 129.1, 128.9, 81.8, 67.8, 60.5, 32.3, 28.7, 19.9, 18.8. IR (neat): ν_{max} 3291, 2369, 1687, 1631, 1433, 1248, 1162, 1039, 742, 698 cm^{-1}.; ESI$^+$ MS m/z 388 [M + Na]$^+$. Anal. ($C_{18}H_{27}N_3O_5$) C, H, N.

*tert-Butyl N-[[(2S)-2-Amino-3-methyl-butanoyl]amino]-carbamate (**12**).* **11** (150 mg, 0.41 mmol) was dissolved in MeOH (5 mL), and 10% Pd/C (15 mg, 10% mass) was added. The reaction flask was flushed three times with hydrogen and stirred, under a hydrogen atmosphere, for 24 h at room temperature. The mixture was then filtered through a pad of Celite, and the cake was washed with methanol (10 mL). The filtrate was evaporated under reduced pressure to give **12** as a white solid (91 mg, 96%); mp 156−158 °C. ^{1}H NMR (300 MHz, $CDCl_3$): δ = 7.82 (bs, 1H), 7.35 (bs, 1H), 3.21 (d, J = 7.3 Hz, 1H), 2.15 (m, 1H), 1.48 (s, 9H), 0.96 (d, J = 8.4 Hz, 3H), 0.83 (d, J = 8.2 Hz, 3H). ^{13}C NMR (75 MHz, $CDCl_3$): δ 173.7, 155.5, 81.5, 59.5, 31.3, 28.2, 19.4, 16.6. IR (neat): ν_{max} 3205, 2256, 1694, 1214 cm $^{-1}$. ESI$^+$ MS m/z 254 [M + Na]$^+$. Anal. $C_{10}H_{21}N_3O_3$ (%) C, H, N.

*tert-Butyl N-[(1S)-1-[[[(2S)-2-(Benzyloxycarbonylamino)-3-methyl-butanoyl]amino]carbamoyl]-2-methyl-propyl]carbamate (**13**).* Compound **11** (1.1 g, 3.01 mmol, 1 equiv) was dissolved in 4 M HCl in dioxane (10 mL) at 0 °C and stirred at room temperature until completely dissolved. The solvent was evaporated off, and the residue was dissolved in DMF (6 mL). Then, *N*-Boc-Val-OH (0.74 g, 3.3 mmol, 1.1 equiv), DIPEA (1.75 g, 12.1 mmol, 4 equiv), HOBt (0.46 g, 3.3 mmol, 1.1 equiv), and EDCI (0.65 g, 3.3 mmol, 1.1 equiv) were successively added and the reaction mixture was stirred at room temperature for 24 h. DMF was removed under reduced pressure, and the residue was dissolved in EtOAc (50 mL). The resulting organic phase was washed successively with 10% aqueous citric acid (10 mL), water (10 mL), 10% aqueous K_2CO_3 (10 mL), and brine (5 mL). The organic phase was dried over $MgSO_4$, filtered, and concentrated under reduced pressure to yield **13** as a white solid (1.14 g, 82% over 2 steps); mp 172−175 °C. ^{1}H NMR (300 MHz, DMSO-d_6): δ 9.91 (s, 1H), 9.84 (s, 1H), 7.36 (m, 5H), 6.73 (s, 1H), 6.69 (s, 1H), 5.05 (s, 2H), 3.89 (m, 2H), 1.92 (m, 2H), 1.38 (s, 9H), 0.89 (m, 12H). ^{13}C NMR (75 MHz, DMSO-d_6): δ 170.1, 169.9, 155.9, 155.3, 137.0, 128.3, 127.7, 127.6, 77.9, 65.35, 58.7, 58.1, 30.4, 30.3, 28.2, 19.1, 18.3. IR (neat): ν_{max} 3224, 1685, 1604, 1531, 1290, 1248, 1167, 1043 cm^{-1}. ESI$^+$ MS m/z 487 [M + Na]$^+$. Anal. $C_{23}H_{36}N_4O_6$ (%) C, H, N.

*Benzyl N-[(1S)-1-[[[(2S)-2-Amino-3-methyl-butanoyl]amino]-carbamoyl]-2-methyl-propyl] Carbamate (**14**).* Same procedure as for **12** from **13**. Product **14** was obtained as a white solid (691 mg, 71%); mp 138−142 °C. ^{1}H NMR (300 MHz, DMSO-d_6): δ 9.93 (s, 1H), 9.82 (s, 1H), 6.61 (s, 1H), 3.93 (m, 2H), 2.01 (m, 2H), 1.48 (s, 9H), 0.92 (m, 12H). ^{13}C NMR (75 MHz, DMSO-d_6): δ 170.2, 169.9, 155.4, 77.4, 58.1, 57.9, 30.6, 30.2, 28.3, 19.2, 19.0. IR (neat): ν_{max} 3276, 2912, 1677, 1607, 1275, 1186, 1089 cm $^{-1}$. ESI$^+$ MS m/z 387 [M + Na]$^+$. Anal. ($C_{15}H_{30}N_4O_4.2H_2O$) C, H, N.

*Phenyl N-(tert-Butoxycarbonylamino)carbamate (**15**).* *tert*-Butyl carbazate (2 g, 15.13 mmol) and pyridine (2.71 mL, 33.29 mmol, 2.2 equiv) were dissolved, with stirring, in CH_2Cl_2 (10 mL) and phenyl chloroformate (2.08 mL, 16.64 mmol, 1.1 equiv) in CH_2Cl_2 (10 mL) was added dropwise over 30 min at 0 °C. The mixture was stirred overnight at room temperature, and CH_2Cl_2 was evaporated off under reduced pressure. The residue was dissolved in EtOAc (400 mL) and washed successively with 10% aqueous citric acid (50 mL), water (100 mL), 10% aqueous K_2CO_3 (50 mL), and water (50 mL). The organic phase was dried over Na_2SO_4, filtered, and concentrated. The resulting crude product was purified by flash chromatography on silica gel and eluted with EtOAc/cyclohexane (20/80), to give **15** as a white powder (3.68 g, 97%); mp 132−134 °C. ^{1}H NMR (300 MHz, DMSO-d_6): δ 7.36 (t, J = 7.7 Hz, 2H), 7.14−7.24 (m, 3H), 7.00 (bs, 1H), 6.50 (bs,

dx.doi.org/10.1021/jm300181j | J. Med. Chem. 2012, 55, 6762−6775

1H), 1.49 (s, 9H). ^{13}C NMR (75 MHz, DMSO-d_6): δ 155.6, 155.3, 150.6, 129.4, 125.8, 121.4, 82.2, 28.2. IR (neat): ν_{max} 3223, 2969, 1758, 1723, 1692, 1519, 1213, 1177, 1025 cm^{-1}. ESI$^+$ MS m/z 275 [M + Na]$^+$. Anal. ($C_{12}H_{16}N_2O_4$) C, H, N.

*tert-Butyl N-(Hydrazinecarbonylamino)carbamate (**16**).* Compound **15** (6.5 g, 25.77 mmol) and hydrazine monohydrate (8.14 mL, 167.5 mmol, 6.5 equiv) in methanol (100 mL) were heated under reflux for 1.5 h, cooled to room temperature, and the solvent removed under reduced pressure. The resulting oily residue was triturated in petroleum ether, and the precipitate obtained was recrystallized from EtOAc/petroleum ether to give **16** as a white solid (3.54 g, 72%); mp 134−136 °C. ^{1}H NMR (300 MHz, DMSO-d_6): δ 8.41 (bs, 1H), 7.80 (s, 1H), 7.34 (s, 1H), 4.04 (bs, 2H), 1.38 (s, 9H). ^{13}C NMR (75 MHz, DMSO-d_6): δ 159.9, 155.9, 78.7, 28.1. IR (neat): ν_{max} 3252, 2974, 1730, 1651, 1229, 1173 cm^{-1}. ESI$^+$ MS m/z 213 [M + Na]$^+$. Anal. ($C_6H_{14}N_4O_3$) C, H, N.

*Phenyl N-[(tert-Butoxycarbonylamino)carbamoylamino]-carbamate (**17**).* Pyridine (678 μL, 8.2 mmol, 2.5 equiv) was added to a suspension of compound **16** (625 mg, 3.3 mmol) in THF (50 mL), and the mixture was stirred until a homogeneous solution was obtained. The solution was then cooled to 0 °C, phenyl chloroformate (458 μL, 3.6 mmol, 1.1 equiv) was added, and the mixture was stirred for 15 min at room temperature. The solvent was evaporated off under reduced pressure, and the residue was dissolved in EtOAc (50 mL). The organic layer was washed sucessively with water (2 × 25 mL), 5% aqueous citric acid (2 × 20 mL), and 10% aqueous K_2CO_3 (2 × 20 mL), dried over Na_2SO_4, filtered, and concentrated under reduced pressure. The residue was purified by flash chromatography on silica gel (EtOAc/cyclohexane, 80/20) to give product **17** as a white solid (923 mg, 91%); mp 173−174 °C. ^{1}H NMR (300 MHz, $CDCl_3$): δ 7.81 (bs, 2H), 7.68 (bs, 1H), 7.09−7.31 (m, 5H), 6.99 (bs, 1H), 1.43 (s, 9H). ^{13}C NMR (75 MHz, $CDCl_3$): δ 158.7, 156.7, 155.8, 150.6, 129.3, 125.7, 121.4, 82.1, 28.1. IR (neat): ν_{max} 3262, 3238, 1712, 1682, 1519, 1489, 1226, 1154 cm^{-1}. ESI$^+$ MS m/z 333 [M + Na]$^+$. Anal. ($C_{13}H_{18}N_4O_5$) C, H, N.

*tert-Butyl N-[[[(1S)-1-Carbamoyl-2-methyl-propyl]-carbamoylamino]carbamoylamino] carbamate (**18**).* Compound **17** (273 mg, 0.88 mmol) and HCl·H-Val-NH$_2$ (151 mg, 0.97 mmol, 1.1 equiv) were dissolved in acetonitrile (17 mL), and triethylamine (741 μL, 5.3 mmol, 6 equiv) was added to the mixture. The mixture was stirred, under an argon atmosphere, for 3 days at room temperature. The solvent was removed under reduced pressure, and the resulting residue was purified by flash chromatography on silica gel (EtOAc/CH_3OH, 90/10) to give product **18** as a white solid (272 mg, 93%); mp 154−156 °C. ^{1}H NMR (300 MHz, DMSO-d_6): δ 8.61 (bs, 1H), 8.13 (s, 2H), 7.77 (s, 1H), 7.37 (bs, 1H), 7.08 (s, 1H), 6.05 (d, J = 8.4 Hz, 1H), 4.00 (dd, J = 8.4, 5.1 Hz, 1H), 1.95−2.02 (m, 1H), 1.41 (s, 9H), 0.87 (d, J = 6.6 Hz, 3H), 0.82 (d, J = 6.6 Hz, 3H). ^{13}C NMR (75 MHz, DMSO-d_6): δ 173.5, 158.6, 158.1, 155.9, 79.0, 57.5, 30.6, 28.1, 19.3, 17.4. IR (neat): ν_{max} 3259, 2969, 1658, 1529, 1241, 1158 cm^{-1}. ESI$^+$ MS m/z 355 [M + 23]$^+$. Anal. ($C_{12}H_{24}N_6O_5$·0.2EtOAc) C, H, N.

*(2S)-2-[(Hydrazinecarbonylamino)carbamoylamino]-3-methyl-butanamide (**19**).* **18** was dissolved in CH_2Cl_2 (0.13 M), an equal volume of TFA was added, and the mixture was stirred at room temperature for 3 h. The solvent was removed, and methanol was added and immediately evaporated off, and then ether was added and again immediately evaporated off to give the corresponding TFA salt of **19**. This was used in the next step without further purification.

*Methyl 3-[[(tert-Butoxycarbonylamino)carbamoylamino]-carbamoylamino]propanoate (**20**).* Same procedure as for **18** from **17** and HCl·H-β-Ala-OCH$_3$. The product **20** was obtained as a white solid (274 mg, 67%); mp 122−124 °C. ^{1}H NMR (300 MHz, DMSO-d_6): δ 8.54 (s, 1H), 8.05 (bs, 2H), 7.68 (s, 1H), 6.20 (br, 1H), 3.61 (s, 3H), 3.25 (dt, J = 11.7, 5.7 Hz, 2H), 2.45 (t, J = 5.7 Hz, 2H), 1.40 (s, 9H). ^{13}C NMR (75 MHz, DMSO-d_6): δ 172.0, 158.4, 155.9, 79.0, 51.3, 35.2, 34.3, 28.1. IR (neat): ν_{max} 3270, 3106, 2936, 1666, 1542, 1161 cm^{-1}. ESI$^+$ MS m/z 342 [M + 23]$^+$. Anal. ($C_{11}H_{21}N_5O_6$·0.15H_2O) C, H, N.

*Methyl 3-[(Hydrazinecarbonylamino)carbamoylamino]-propanoate (**21**).* Same procedure as for **19** from **20**. The corresponding TFA salt of **21** was used in the next step without further purification.

*tert-Butyl N-[(Methylcarbamoylamino)carbamoylamino]-carbamate (**22**).* Same procedure as for **18** from **17** and HCl·NH_2CH_3. The product **22** was obtained as a white solid (84 mg, 70%); mp 232−234 °C. ^{1}H NMR (300 MHz, DMSO-d_6): δ 8.54 (bs, 1H), 8.05 (bs, 2H), 7.61 (s, 1H), 6.07 (bs, 1H), 2.56 (d, J = 4.5 Hz, 3H), 1.40 (s, 9H). ^{13}C NMR (75 MHz, DMSO-d_6): δ 159.1, 158.4, 155.9, 79.0, 28.1, 26.1. IR (neat): ν_{max} 3272, 3106, 2936, 1665, 1474, 1159 cm^{-1}. ESI$^+$ MS m/z 270 [M + 23]$^+$. Anal. ($C_8H_{17}N_5O_4$) C, H, N.

*1-Amino-3-(methylcarbamoylamino)urea (**23**).* Same procedure as for **19** from **22**. The TFA salt of **23** was used in the next step without further purification.

*tert-Butyl N-(Acetamidocarbamoylamino)carbamate (**24**).* **16** (3 g, 15.7 mmol) was dissolved in dry THF (180 mL) with stirring, and acetic anhydride (7.45 mL, 78.8 mmol, 5 equiv) was added dropwise. The mixture was heated under reflux for 1.5 h, the solvent was removed under reduced pressure, and the resulting residue was triturated in CH_2Cl_2. The precipitate obtained was washed with petroleum ether to yield compound **24** as a white solid (3.5 g, 96%); mp 118−120 °C. ^{1}H NMR (300 MHz, DMSO-d_6): δ 9.46 (s, 1H), 8.51 (s, 1H), 8.09 (s, 1H), 8.07 (s, 1H), 1.80 (s, 3H), 1.39 (s, 9H). ^{13}C NMR (75 MHz, DMSO-d_6): δ 168.7, 157.7, 155.8, 78.8, 28.05, 20.56. IR (neat): ν_{max} 3301, 1663, 1521, 1238, 1158 cm^{-1}. ESI$^+$ MS m/z 255 [M + Na]$^+$. Anal. ($C_8H_{16}N_4O_4$·0.15H_2O) C, H, N.

*1-Acetamido-3-amino-urea (**25**).* Compound **24** (88 mg, 0.38 mmol) was dissolved in 4 M HCl in dioxane (4 mL) and stirred at room temperature for 2 h. The solvent was removed, and the HCl salt of **25** was obtained as a white solid (64 mg, 100%) and used in the next step without further purification.

*tert-Butyl N-[(1S)-1-[(Acetamidocarbamoylamino)carbamoyl]-2-methyl-propyl]carbamate (**26**).* **25** (163 mg, 0.97 mmol) and *N*-Boc-Val-OH were dissolved in DMF (15 mL) with stirring at 0 °C, and DIPEA (1.0 mL, 5.82 mmol, 10 equiv), HBTU (440 mg, 1.16 mmol, 1.2 equiv), and HOBt (145 mg, 1.07 mmol, 1.1 equiv) were added successively. The reaction mixture was stirred under argon at room temperature for 24 h. The DMF was removed under reduced pressure, and the residue was dissolved in EtOAc (200 mL). The organic phase was washed with water (2 × 50 mL) and concentrated under reduced pressure. The aqueous phase was then concentrated and extracted twice with EtOAc because compound **26** is extremely soluble in water. The oily crude product was purified by flash chromatography on silica gel (EtOAc 100% to EtOAc/CH_3OH, 10/1) to give product **26** as a white solid (150 mg, 46%); mp 110−112 °C. ^{1}H NMR (300 MHz, DMSO-d_6): δ 9.65 (br, 1H), 9.50 (s, 1H), 8.32 (br, 1H), 8.03 (s, 1H), 6.73 (d, J = 8.1 Hz, 1H), 3.79−3.74 (m, 1H), 1.95−1.87 (m, 1H), 1.80 (s, 3H), 1.37 (s, 9H), 0.89−0.83 (m, 6H). ^{13}C NMR (75 MHz, DMSO-d_6): δ 171.1, 168.8, 157.2, 78.0, 58.2, 30.2, 28.1, 20.5, 19.0, 18.3. IR (neat): ν_{max} 3261, 1668, 1507, 1244, 1161 cm^{-1}. ESI$^+$ MS m/z 354 [M + Na]$^+$. HRMS calcd for $C_{13}H_{25}N_5O_5$ + Na (354.1753), found 354.1752.

*1-Acetamido-3-[[(2S)-2-amino-3-methyl-butanoyl]amino]urea (**27**).* Same procedure as for **25** from **26**. The HCl salt of **27** was used in the next step without further purification.

*tert-Butyl N-[3-[2-(Acetamidocarbamoyl)hydrazino]-3-oxo-propyl]carbamate (**28**).* Same procedure as for **26** from **25** and Boc-β-Ala-OH. The product **28** was obtained as a light-brown solid (95 mg, 12%); mp 145−147 °C. ^{1}H NMR (400 MHz, DMSO-d_6): δ 9.54 (s, 1H), 9.49 (s, 1H), 8.21 (br, 2H), 6.77−6.74 (m, 1H), 3.17−3.09 (m, 2H), 2.28−2.22 (m, 2H), 1.80 (s, 3H), 1.37 (s, 9H). ^{13}C NMR (100 MHz, DMSO-d_6): δ 174.0, 173.2, 160.1, 158.3, 80.2, 37.6, 35.2, 28.7, 20.6. IR (neat): ν_{max} = 3245, 1659, 1511, 1164. ESI$^-$ MS m/z 302. Anal. ($C_{11}H_{21}N_5O_5$) C, H, N.

*1-Acetamido-3-(3-aminopropanoylamino)urea (**29**).* Same procedure as for **25** from **28**. The HCl salt of **29** was used in the next step without further purification.

dx.doi.org/10.1021/jm300181j | J. Med. Chem. 2012, 55, 6762−6775

*tert-Butyl N-[(1S)-1-[(Acetamidocarbamoylamino)carbamoyl]-5-(phenoxycarbonylamino) pentyl]carbamate (**30**).* Same procedure as for **26** from **25** and *Nα*-Boc-*Nε*-*Z*-Lys-OH. The product **30** was obtained as a white solid (88 mg, 30%); mp 129−131 °C. ^{1}H NMR (300 MHz, DMSO-d_6): δ 9.65 (br, 1H), 9.49 (br, 1H), 8.32 (br, 1H), 8.04 (s, 1H), 7.37−7.32 (m, 5H), 7.24 (t, J = 5.2 Hz, 1H), 6.87 (d, J = 7.5 Hz, 1H), 5.00 (s, 2H), 3.92−3.85 (m, 1H), 2.99−2.93 (m, 2H), 1.80 (s, 3H), 1.61−1.47 (m, 2H), 1.40−1.24 (m, 13H). ^{13}C NMR (75 MHz, DMSO-d_6): δ 175.3. 173.3, 160.0, 159.1, 158.3, 138.6, 129.6, 129.1, 128.9, 81.0, 67.5, 55.1, 41.6, 32.6, 30.6, 28.9, 24.0, 20.7. IR (neat): ν_{max} 3307, 1665, 1522, 1246, 1167 cm^{-1}. ESI$^-$ MS m/z 493 [M − H]$^-$; Anal. ($C_{22}H_{34}N_6O_7\cdot 1H_2O$) C, H, N.

*tert-Butyl N-[(1S)-1-[(Acetamidocarbamoylamino)carbamoyl]-5-amino-pentyl]carbamate (**31**).* Same procedure as for **12** from **30**. The product **31** was obtained as a white solid (164 mg, 100%); mp 150−160 °C. ^{1}H NMR (300 MHz, CD_3OD): δ 4.01 (t, J = 6.3 Hz, 1H), 2.69 (t, J = 6.7 Hz, 2H), 1.98 (s, 3H), 1.83−1.61 (m, 2H), 1.56−1.45 (m, 13H). ^{13}C NMR (75 MHz, CD_3OD): δ 174.6, 173.1, 159.9, 158.2, 80.8, 55.0, 41.9, 32.6, 32.4, 28.7, 23.9, 20.5. IR (neat): ν_{max} 3289, 2977, 1663, 1508, 1368, 1162 cm^{-1}. ESI$^+$ MS m/z 361 [M + H]$^+$, 383 [M + Na]$^+$.

*Synthesis of Molecule (**33**).* **32** (982 mg, 1.49 mmol, 1 equiv) was dissolved, with stirring, in DMF (55 mL) and DIPEA (0.39 mL, 2.24 mmol, 1.5 equiv), **12** (449 mg, 1.94 mmol, 1.3 equiv) and HBTU (680 mg, 1.794 mmol, 1.2 equiv) were added successively. The mixture was stirred at room temperature for 5 days, and the DMF was removed under reduced pressure. A solid was precipitated from the oily crude with CH_2Cl_2. This was washed successively with CH_2Cl_2, aqueous HCl 0.1 M, aqueous $NaHCO_3$, brine, and CH_2Cl_2. Product **33** was obtained as a white solid (986 mg, 76%); mp 220−222 °C. ^{1}H NMR (300 MHz, DMSO-d_6): δ 9.70 (s, 1H), 8.73 (s, 1H), 8.28 (bs, 1H), 7.94−8.00 (m, 3H), 7.70 (d, J = 9.0 Hz, 2H), 7.17 (s, 2H), 6.97 (d, J = 9.0 Hz, 2H), 4.35−4.43 (m, 1H), 4.12−4.22 (m, 3H), 4.05 (t, J = 6.3 Hz, 4H), 3.60 (s, 3H), 2.32−2.41 (m, 4H), 1.89−2.05 (m, 7H), 1.53−1.66 (m, 1H), 1.41−1.46 (m, 2H), 1.38 (s, 9 H), 0.80−0.90 (m, 24 H). ^{13}C NMR (75 MHz, DMSO-d_6): δ 172.1, 171.6, 171.5, 170.8, 170.6, 156.9, 155.0, 135.6, 128.8, 123.6, 115.8, 106.0, 78.9, 66.8, 57.7, 57.2, 55.9, 51.5, 50.7, 40.6, 31.5, 31.4, 30.6, 30.1, 29.8, 27.9, 24.9, 24.9, 24.0, 22.8, 21.5, 19.1, 18.7, 18.2, 18.1, 18.0. IR (neat): ν_{max} 3279, 2956, 2365, 1740, 1635, 1535, 1210, 1162 cm^{-1}. ESI$^+$ MS m/z 894 [M + Na]$^+$. Anal. ($C_{45}H_{70}N_6O_{11}\cdot 3H_2O$) C, H, N.

Enzymatic Studies. The fluorogenic substrate for PR and mutated proteases was DABCYL-γ-abu-Ser-Gln-Asn-Tyr-Pro-Ile-Val-Gln-EDANS [DABCYL, 4-(4′-dimethylaminophenylazo)benzoyl; γ-abu, γ-amino butyric acid. EDANS, 5-[(2-aminoethyl)amino]naphthalene-1-sulfonic acid)], was purchased from Bachem (Germany). 1-Anilino-8-naphthalene sulfonate (ANS) was from Sigma-Aldrich, and saquinavir and amprenavir were from the NIH (USA). The fluorogenic pepsin substrate Arg-Glu(EDANS)-Ile-His-Pro-Phe-His-Leu-Val-Ile-His-Thr-Lys(DABCYL)-Arg, the renin substrate Abz-Thr-Ile-Nle-(*p*-NO_2-Phe)-Gln-Arg-NH_2, and recombinant renin and pepsin were purchased from Sigma−Aldrich. Other reagents and solvents were purchased from commercial sources. Absorbance measurements were made with a Perkin-Elmer LS 50B spectrophotometer. Fluorescence intensities were measured in a BMG Fluostar microplate reader.

Wild-Type and Mutated Proteases. The HIV-1 proteases (PR, MDR-HM, and ANAM-11[22]) used in this study were expressed and purified as described before.[14] They were produced in *Escherichia coli* using the expression vector pET-9 and the host bacterium strain Rosetta (DE3)pLysS. The protease domain (PR) has five protective mutations, Q7K, L33I, L63I to minimize the autoproteolysis of the protease and C67A and C95A to prevent cysteine−thiol oxidation. The multimutated HIV-1 proteases ANAM-11 and MDR-HM contain 11 mutations (L10I/M36I/S37D/M46I/R57K/L63P/A71 V/G73S/I84 V/L90M/I93L) (ref 31) and six mutations (L10I/M46I/I54 V/V82A/I84 V/L90M) (ref 30), respectively.

Enzyme and Inhibition Assays. The proteolytic activities of PR and mutated proteases were determined fluorometrically using the fluorogenic substrate DABCYL-γ-abu-SQNYPIVQ-EDANS (λ_{ex} = 340 nm; λ_{em} = 490 nm) in 100 mM sodium acetate, 1 mM EDTA, and 1 M NaCl at pH 4.7 and 30 °C (final volume, 150 μL). The substrate and the compound(s) were first dissolved in DMSO. The final DMSO concentration was kept at 3% (v/v). The mechanism of inhibition and the corresponding kinetic constants K_{id} (dimerization inhibition) or K_{ic} (competitive inhibition) were determined using Zhang−Poorman kinetic analysis.[11] Kinetic experiments were carried out at a constant substrate concentration (5.2 μM) with at least six enzyme concentrations (5.33−18.6 nM) and inhibitor concentrations from 0.5 to 28 μM. The experimental data were fitted to the appropriate equations according to ref 14. All experiments were performed at least in triplicate.

Fluorescent Probe Binding. Hydrophobic ANS preferentially binds to the hydrophobic surfaces of proteins. ANS emission spectra were measured using an excitation wavelength of 370 nm and an emission wavelength of 470 nm with bandwidths of 10 and 5 nm, respectively (Perkin-Elmer LS 50B spectrofluorometer) as described in ref 21. PR (350 nM) was dissolved in the assay buffer (100 mM sodium acetate, 1 M NaCl, 1 mM EDTA, pH 4.7) and incubated at 25 °C with or without inhibitor (5 μM; acetylpeptsatin, saquinavir, compounds **1**, **2**, **3**, **4**, and **P1**). ANS (2 μL, final concentrations: 10−60 μM) was then added. In all cases, the final DMSO concentration was 0.2% (v/v). Each fluorescence measurement was made five times and averaged. The intrinsic fluorescence of PR, acetylpepstatin, saquinavir, and compounds **1**, **2**, **3**, **4**, and **P1** was negligible under the experimental conditions used.

Evaluation of Metabolic Stability. The stability of inhibitors in RPMI (Roswell Park Memorial Institute medium) culture medium containing 20% fetal calf serum was assessed by studying their kinetics of breakdown at 37 °C for up to 2 days. Incubations were terminated by adding ethanol. The mixture was poured at 4 °C and centrifuged (10000 rpm for 10 min). Aliquots of the clear supernatant were injected onto the HPLC column (Waters E600). The half-life of breakdown was obtained by least-squares linear regression analysis of the semilogarithmic plot of remaining inhibitor concentration versus incubation time.

Inhibition of Renin and Pepsin. The proteolytic activity of renin was determined fluorometrically using the fluorogenic substrate Arg-Glu(EDANS)-Ile-His-Pro-Phe-His-Leu-Val-Ile-His-Thr-Lys-(DABCYL)-Arg (K_m = 3.3 μM). Assays were performed in 50 mM Tris−HCl, 100 mM NaCl, 1 mM EDTA, pH 8.0, and a substrate concentration of 5 μM (λ_{ex}= 340 nm, λ_{em} = 500 nm).

The proteolytic activity of pepsin from porcine gastric mucosa was determined fluorometrically using the fluorogenic substrate Abz-Thr-Ile-Nle-(p-NO_2-Phe)-Gln-Arg-NH_2 (K_m = 13.3 μM). Assays were performed in 10 mM NaHCOO, pH 3.5, and a substrate concentration of 20 μM (λ_{ex}= 337 nm, λ_{em} = 410 nm).

Molecular Modeling. *Models of Molecular Tongs−PR Complexes.* Models of molecules **1**−**10** were built using CORINA 3.44 software[33] and then energy minimized (by 2000 steps) using the Powell method as implemented in SYBYL 8.0 software.[34] Dihedral angles were then adjusted so that each molecule was superimposed over the backbone of chain B (subsequently removed) from the crystallographic structure of HIV protease 7HVP (PDB accession code).

The geometries of the resulting complexes were optimized by energy minimization using the AMBER7 FF02 force field as implemented in SYBYL to relax the structure and to remove steric bumps. The minimizations were carried out by 1000 steps of steepest descent followed by a conjugate gradient minimization until the rms gradient of the potential was lower than 0.05 kcal·mol^{-1}·Å^{-1}. A distance-dependent (ε = 4r) dielectric function was used. Analysis of the complex models involved the study of the hydrogen bond network and counting of favorable interactions.

Estimation of Accessible Surface Areas and clogP. Three-dimensional coordinates for free compounds **1**−**10** and **P1** generated with CORINA software were energy-minimized with OPLS_2005 force field as implemented in MacroModel 9.9.[35] Solvent-accessible surface areas and clogP were calculated for these models with QikProp 3.4.[36]

dx.doi.org/10.1021/jm300181j | J. Med. Chem. 2012, 55, 6762−6775

■ ASSOCIATED CONTENT

Supporting Information

Putative complexes between the PR monomer and peptidomimetic molecular tongs **1**−**9**. Purity: HPLC chromatograms of molecular tongs **1**−**9** and analytical data of compounds. Metabolic stability: HPLC chromatograms. This material is available free of charge via the Internet at http://pubs.acs.org.

■ AUTHOR INFORMATION

Corresponding Author

*For S.O.: phone, 33(0)-146835743; fax, 33(0)146835740; E-mail, sandrine.ongeri@u-psud.fr. For M.R-R.: phone, 33(0)-144275078; fax, 33(0)-144275140; E-mail, michele.reboud@upmc.fr.

Notes

The authors declare no competing financial interest.

■ ACKNOWLEDGMENTS

We thank Claire Troufflard (UMR 8076, Faculty of Pharmacy at Châtenay-Malabry) for the NMR experiments, Christine Philippe for their help with the syntheses, and Lixian Qin for carrying some ANS experiments. Financial support for A.S.M.R., A.V., and N.K. (Marie Curie Early Stage training Fellowship of the European Community's Sixth Framework Programme: contract MESTCT-2004-515968) was provided by the European Community. The Ministère de la Recherche et des Technologies (MRT) provided financial support for L.D., and the Italian Research Ministery provided finances for R.F. We thank Prof. Ernesto Freire of the Department of Biology and Biocalorimetry Center, Johns Hopkins University, Baltimore, MD, for the generous gift of the plasmid encoding the ANAM-11 mutant. Saquinavir was obtained through the NIH AIDS Research and Reference Reagent Program, Division of AIDS, NIAID, NIH. The English text was edited by Dr Owen Parkes.

■ ABBREVIATIONS USED

PR, HIV-1 protease; PIs, PR inhibitors; EDCI, 1-ethyl-3-(3-dimethylaminopropyl) carbodiimide; HOBt, *N*-hydroxybenzotriazole; Boc, *tert*-butyloxycarbonyl; HBTU, *O*-benzotriazole-*N*,*N*,*N*′,*N*′-tetramethyl-uronium-hexafluoro-phosphate; ANS, 1-anilino-8-naphthalene sulfonate; DABCYL, 4-(4′-dimethylaminophenylazo)benzoyl; γ-abu, γ-amino butyric acid; EDANS, 5-[(2-aminoethyl)amino]naphthalene-1-sulfonic acid)}; EDTA, ethylenediaminetetraacetic acid; ANAM-11, multimutated HIV-1 protease containing 11 mutations; MDR-HM, multimutated HIV-1 protease containing six mutations; rms, root-mean-square

■ REFERENCES

(1) Orozlan, S.; Luftig, R. B. Retroviral proteinases. *Curr. Top. Microbiol. Immunol.* **1990**, *157*, 153−185.

(2) Kohl, N. E.; Emini, E. A.; Schleif, W. A.; Davis, L. J.; Heimbach, J. C.; Dixon, R. A.; Scolnick, E. M.; Sigal, I. S. Active human immunodeficiency virus protease is required for viral infectivity. *Proc. Natl. Acad. Sci. U.S.A.* **1988**, *85*, 4686−4690.

(3) Carr, A. Toxicity of antiretroviral therapy and implications for drug development. *Nature Rev. Drug Discovery* **2003**, *2*, 624−634.

(4) (a) D'Aquila, R. T.; Schapiro, J. M.; Brun-Vezinet, F.; Clotet, B.; Conway, B.; Demeter, L. M.; Grant, R. M.; Johnson, V. A.; Kuritzkes, D. R.; Loveday, C.; Shafer, R. W.; Richman, D. D. Drug Resistance Mutations in HIV-1. *Top. HIV Med.* **2002**, *10*, 21−25. (b) De Clercq, E. Antivirals and antiviral strategies. *Nature Rev. Microbiol.* **2004**, *2*, 704−720.

(5) Ishima, R.; Ghirlando, R.; Tozser, J.; Gronenborn, A. M.; Torchia, D. A.; Louis, J. M. Folded monomer of HIV-1 protease. *J. Biol. Chem.* **2001**, *276*, 49110−49116.

(6) Todd, M. J.; Semo, N.; Freire, E. The structural stability of the HIV-1 protease. *J. Mol. Biol.* **1998**, *283*, 475−488.

(7) Gustchina, A.; Weber, I. T. Comparative analysis of the sequences and structures of HIV-1 and HIV-2 proteases. *Proteins* **1991**, *10*, 325−329.

(8) (a) Boggetto, N.; Reboud-Ravaux, M. Dimerization inhibitors of HIV-1 protease. *Biol. Chem.* **2002**, *383*, 1321−1324. (b) Banwarth, L.; Reboud-Ravaux, M. An alternative strategy for inhibiting multidrug-resistant mutants of the dimeric HIV-1 protease by targeting the subunit interface. *Biochem. Soc. Trans.* **2007**, *35*, 551−554.

(9) Hamacher, K Relating sequence evolution of HIV1-protease to its underlying molecular mechanics. *Gene* **2008**, *422*, 30−36.

(10) Schramm, H. J.; Nakashima, H.; Schramm, W.; Wakayama, H.; Yamamoto, N. HIV-1 reproduction is inhibited by peptides derived from the N- and C-termini of HIV-1 protease. *Biochem. Biophys. Res. Commun.* **1991**, *179*, 847−851.

(11) Zhang, Z. Y.; Poorman, R. A.; Maggiora, L. L.; Heinrikson, R. L.; Kezdy, F. J. Dissociative inhibition of dimeric enzymes. Kinetic characterization of the inhibition of HIV-1 protease by its COOH-terminal tetrapeptide. *J. Biol. Chem.* **1991**, *266*, 15591−15594.

(12) Franciskovich, J.; Houseman, K.; Mueller, R.; Chiemlevski, J. A systematic evaluation of the inhibition of HIV-1 protease by its C-terminal and N-terminal peptides. *Bioorg. Med. Chem. Lett.* **1993**, *3*, 765−768.

(13) Schramm, H. J.; de Rosny, E.; Reboud-Ravaux, M.; Buttner, J.; Dick, A.; Schramm, W. Lipopeptides as dimerization inhibitors of HIV-1 protease. *Biol. Chem.* **1999**, *380*, 593−596.

(14) Dumond, J.; Boggetto, N.; Schramm, H. J.; Schramm, W.; Takahashi, M.; Reboud-Ravaux, M. Thyroxine-derivatives of lipopeptides: bifunctional dimerization inhibitors of immunodeficiency virus-1 protease. *Biochem. Pharmacol.* **2003**, *65*, 1097−1102.

(15) Bannwarth, L.; Rose, T.; Dufau, L.; Vanderesse, R.; Dumond, J.; Jamart-Gregoire, B.; Pannecouque, C.; De Clercq, E.; Reboud-Ravaux, M. Dimer disruption and monomer sequestration by alkyl tripeptides are successful strategies for inhibiting wild-type and multidrug-resistant mutated HIV-1 proteases. *Biochemistry* **2009**, *48*, 379−387.

(16) Breccia, P.; Boggetto, N.; Perez-Fernandez, R.; Van Gool, M.; Takahashi, M.; Rene, L.; Prados, P.; Badet, B.; Reboud-Ravaux, M.; de Mendoza, J. Dimerization inhibitors of HIV-1 protease based on a bicyclic guanidinium subunit. *J. Med. Chem.* **2003**, *46*, 5196−5207.

(17) Zutshi, R.; Franciskovich, J.; Slultz, M.; Schwetizer, B.; Bishop, P.; Wilson, M.; Chmielewski, J. Targeting the dimerization interface of HIV-1 protease: inhibition with cross-linked interfacial peptides. *J. Am. Chem. Soc.* **1997**, *119*, 4841−4845.

(18) Ulysse, L. G.; Chiemlevski, J. Restricting the flexibility of crosslinked, interfacial peptide inhibitors of HIV-1 protease. *Bioorg. Med. Chem. Lett.* **1998**, *8*, 3281−3286.

(19) Koh, Y.; Matsumi, S.; Das, D.; Amano, M.; Davis, D. A.; Li, J.; Leschenko, S.; Baldridge, A.; Shioda, T.; Yarchoan, R.; Ghosh, A. K.; Mitsuya, H. Potent inhibition of HIV-1 replication by novel non-peptidyl small molecule inhibitors of protease dimerization. *J. Biol. Chem.* **2007**, *282*, 28709−28720.

(20) Bouras, A.; Boggetto, N.; Benatalah, Z.; de Rosny, E.; Sicsic, S.; Reboud-Ravaux, M. Design, synthesis, and evaluation of conformationally constrained tongs, new inhibitors of HIV-1 protease dimerization. *J. Med. Chem.* **1999**, *42*, 957−962.

(21) Merabet, N.; Dumond, J.; Collinet, B.; Van Baelinghem, L.; Boggetto, N.; Ongeri, S.; Ressad, F.; Reboud-Ravaux, M.; Sicsic, S. New constrained "molecular tongs" designed to dissociate HIV-1 protease dimer. *J. Med. Chem.* **2004**, *47*, 6392−6400.

(22) Bannwarth, L.; Kessler, A.; Pethe, S.; Collinet, B.; Merabet, N.; Boggetto, N.; Sicsic, S.; Reboud-Ravaux, M.; Ongeri, S. Molecular tongs containing amino acid mimetic fragments: new inhibitors of

wild-type and mutated HIV-1 protease dimerization. *J. Med. Chem.* **2006**, *49*, 4657−4664.
(23) Vidu, A.; Dufau, L.; Bannwarth, L.; Soulier, J. L.; Sicsic, S.; Piarulli, U.; Reboud-Ravaux, M.; Ongeri, S. Toward the First Nonpeptide Molecular Tong Inhibitor of Wild-Type and Mutated HIV-1 Protease Dimerization. *ChemMedChem.* **2010**, *11*, 1899−1906.
(24) (a) Han, H.; Janda, K. D. Azatides: solution and liquid phase synthesis of a new peptidomimetic. *J. Am. Chem. Soc.* **1996**, *118*, 2539−2544. (b) Wang, D.; Pechar, M.; Weije, L.; Kopeckova, P.; Brömme, D.; Kopecek, J. Inhibition of cathepsin K with lysosomotropic macromolecular inhibitors. *Biochemistry* **2002**, *41*, 8849−8859.
(25) (a) Abbruscato, T. J.; Williams, S. A.; Misicka, A.; Lipkowski, A. W.; Hruby, V. J.; Davis, T. P. Blood-to-central nervous system entry and stability of biphalin, a unique double-enkephalin analog, and its halogenated derivatives. *J. Pharmacol. Exp. Ther.* **1996**, *279*, 1049−1057. (b) Witt, K. A. CNS drug delivery: opioid peptides and the blood−brain barrier. *AAPS J.* **2006**, *8* (Article 9), E76−E88.
(26) Zhao, X.; Wang, X. Z.; Jiang, X. K.; Chen, Y. Q.; Li, Z. T.; Chen, G. J. Hydrazide-based quadruply hydrogen-bonded heterodimers. Structure, assembling selectivity, and supramolecular substitution. *J. Am. Chem. Soc.* **2003**, *125*, 15128−15139.
(27) Hou, J. L.; Shao, X. B.; Chen, G. J.; Zhou, Y. X.; Jiang, X. K.; Li, Z. T. Hydrogen bonded oligohydrazide foldamers and their recognition for saccharides. *J. Am. Chem. Soc.* **2004**, *126*, 12386−12394.
(28) Feng, D.-J.; Wang, P.; Li, X.-Q.; Li, Z.-T. Self-assembly of hydrazide-based heterodimers driven by hydrogen bonding and donor−acceptor interaction. *Chin. J. Chem.* **2006**, *24*, 1200−1208.
(29) Gray, C. J.; Ireson, J. C.; Parker, R. C. Preparation and properties of some α-aza-amino-acid derivatives, their possible use in peptide synthesis. *Tetrahedron* **1977**, *33*, 739−743.
(30) Ohtaka, H.; Schön, A.; Freire, E. Multidrug Resistance to HIV-1 Protease Inhibition Requires Cooperative Coupling between Distal Mutations. *Biochemistry* **2003**, *42*, 13659−13666.
(31) Muzammil, S.; Ross, P.; Freire, E. A Major Role for a Set of Non-Active Site Mutations in the Development of HIV-1 Protease Drug Resistance. *Biochemistry* **2003**, *42*, 631−638.
(32) Stryer, L. The Interaction of a Naphthalene Dye with Apomyoglobin and Apohemoglobin. A Fluorescent Probe of Nonpolar Binding Sites. *J. Mol. Biol.* **1965**, *13*, 482−495.
(33) (a) Sadowski, J.; Gasteiger, J.; Klebe, G. Comparison of Automatic Three-Dimensional Model Builders Using 639 X-Ray Structures. *J. Chem. Inf. Comput. Sci.* **1994**, *34*, 1000−1008. (b) The 3D structure generator CORINA is available from Molecular Networks GmbH, Erlangen, Germany.
(34) *SYBYL 8.0*; Tripos International: 1699 South Hanley Rd., St. Louis, Missouri, 63144, USA.
(35) *MacroModel*, version 9.9; Schrödinger, LLC: New York, 2011.
(36) *QikProp*, version 3.4; Schrödinger, LLC: New York, 2011.